

**A STUDY ON THE VISCOUS BEHAVIOR OF Al_2O_3 - H_2O ,
ETHYLENE GLYCOL BASED NANOFUIDS**

**A
DISSERTATION**

**SUBMITTED IN PARTIAL FULFILLMENT OF THE REQUIREMENTS
FOR THE AWARD OF THE DEGREE OF**

**MASTER OF ENGINEERING
IN
THERMAL ENGINEERING**

Submitted by:

JASKARAN SINGH

Roll No: 801083010

Under the supervision of:

Mr. KUNDAN LAL

Assistant Professor, MED

TU, Patiala-147004



MECHANICAL ENGINEERING DEPARTMENT

THAPAR UNIVERSITY

PATIALA – 147004

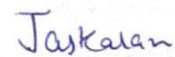
2012

CERTIFICATE

This is to certify that the work which is being presented in this thesis report entitled "A Study on the Viscous Behavior of $\text{Al}_2\text{O}_3 - \text{H}_2\text{O}$, Ethylene Glycol Based Nanofluids", in partial fulfillment of the requirement for the award of the master degree in Master of Engineering (Thermal Engineering) submitted in the Mechanical Engineering Department, Thapar University, Patiala, is a authentic record of the initial work carried out by me under the guidance of **Mr. Kundan Lal, Assistant Professor, MED Thapar University, Patiala.**

The matter embodied in this report has not been submitted in part or full to any other university or institute for the award of any degree.


Dated: 5th July 2012

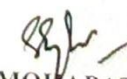

Jaskaran Singh

This is to certify that the above declaration made by the student concerned is correct to the best of my knowledge and belief.


Mr. KUNDAN LAL
Assistant Professor, MED
Thapar University, Patiala.

Countersigned by:


Dr. AJAY BATISH
Professor and Head, MED
Thapar University, Patiala.


Dr. S.K. MOHAPATRA
Dean of Academic Affairs
Thapar University, Patiala

ACKNOWLEDGEMENT

I express my sincere gratitude to **Mr. Kundan Lal, Assistant Professor, Mechanical Engineering Department Thapar University, Patiala**, for their valuable guidance, proper advice and constant encouragement in my thesis work.

I do not find enough words with which I can express my feeling of thanks to the entire faculty and staff of **Mechanical Engineering Department Thapar University, Patiala**, for their help, inspiration and moral support. My special thanks are due to my family members and friends who constantly encouraged me to complete this study.

Jaskaran

JASKARAN SINGH

ABSTRACT

Nanofluid is a colloidal solution in which nanoparticles (1 to 100 nm) are suspended in the base fluid. It has been found that they have potential use in cooling applications because of their improved heat removal capabilities. Since most of the cooling methods used, involve forced circulation of the coolant, therefore modifications in properties of fluids which can result in an increased pumping power requirement is a critical issue. As it is evident that, viscosity is one of the thermo-physical property of the fluid which significantly affects the pumping power as well as the convective heat transfer performance of the coolants, as the Prandtl number and Reynolds number are functions of viscosity. In most of the cold countries, the minimum ambient temperature dips to about -30°C to -40°C and the coolants used must have lower freezing points. Therefore, the ideal coolant is one which will have a lower freezing point and a lower viscosity.

Pure ethylene glycol has a freezing point of about -12°C , but when it is mixed with water, the freezing point of the mixture gets depressed to -45°C . Pure water has a freezing point of 0°C , therefore it cannot be used in cold countries. Water has a lower viscosity as compared to the ethylene glycol and when water is mixed with ethylene glycol, the resulting mixture has a viscosity lower than pure ethylene glycol. Therefore, 60:40 ratio mixture of ethylene glycol and water by volume has a lower freezing point and a lower viscosity as compared to the pure ethylene glycol. This is the reason for using one of the base fluids as a mixture of water and ethylene glycol.

In the present research work, the effect of factors such as volumetric concentration of the nanoparticles, temperature, shear rate on the viscous behavior of Al_2O_3 nanoparticles in two base fluids- (Ethylene Glycol) and (a mixture of Water and Ethylene Glycol mixed in the ratio of 60:40 by volume) has been studied. Very low volumetric concentrations of 0%, 0.005%, 0.01%, 0.05%, and 0.1% of Al_2O_3 nanoparticles have been used in this experimental work. The Al_2O_3 nanoparticles having an average particle size of 40 nm are used in this work. The temperature is varied from 25°C to 50°C and shear rate is varied from 38 to 190 (1/s). The Rheological behavior i.e. Newtonian/ Non- Newtonian behavior is also studied.

INDEX

CONTENTS	PAGE
CERTIFICATE	i
ACKNOWLEDGEMENT	ii
ABSTRACT	iii
INDEX	iv
LIST OF FIGURES	vi
LIST OF TABLES	ix
ACRONYMES	x
CHAPTER 1. INTRODUCTION	1-10
1.1 Nanofluids	1
1.2 Importance of Nanofluids	1
1.3 Preparation of Nanofluids	2
1.3.1 Two step process	2
1.3.2 Single step process	3
1.4 Materials for Nanofluids	3
1.5 Viscosity of Nanofluids	4
1.5.1 Viscosity	4
1.5.2 Newtonian behavior	5
1.6 Factors Effecting the Viscosity of Nanofluids	5
1.6.1 Effect of nanoparticles used	5
1.6.2 Effect of sonication time	6
1.6.3 Effect of base fluid & surfactants	7
1.6.4 Effect of pH value	8
1.6.5 Effect of concentration	9
1.6.6 Effect of temperature	9
1.7 Objectives	10
CHAPTER 2. LITERATURE REVIEW	11-21
2.1 Viscous Behavior of Different Nanofluids	11
2.2 Factors Effecting Viscosity	15
2.3 Theoretical Models used to Predict the Dynamic Viscosity of	18

CHAPTER 3. EXPERIMENTAL SETUP	22-27
3.1 Transmission Electron Microscope (TEM)	22
3.2 Scanning Electron Microscope (SEM)	22
3.3 X- Ray Diffraction (XRD)	23
3.4 Sonicator	24
3.5 Viscometer	26
CHAPTER 4. EXPERIMENTAL WORK, RESULTS & DISCUSSIONS	28-53
4.1 Methodology	28
4.2 Characterization	30
4.3 Al ₂ O ₃ - EG Based Nanofluids	33
4.4 Al ₂ O ₃ - (EG + H ₂ O) Based Nanofluids	41
4.5 Comparison of (EG) and (EG + H ₂ O) based nanofluids	50
CHAPTER 5. CONCLUSIONS AND FUTURE SCOPE	54-55
5.1 Conclusions	54
5.2 Future Scope	55
REFERENCES	56-58
ANNEXURES (I-X)	59-68

LIST OF FIGURES

NO.	DESCRIPTION	PAGE
1.1	Interaction potential energy curve	6
1.2	Surface charging of nanoparticles	7
1.3	Steric repulsions caused by the surfactants	8
2.1	Effect of nanoparticles size on the viscosity of Al ₂ O ₃ - H ₂ O based nanofluids	15
2.2	Variation of effective viscosity of Al ₂ O ₃ - water nanofluids with temperature at different nanoparticle volume fractions	16
2.3	Variation of the viscosity with pH of the Al ₂ O ₃ - H ₂ O nanofluid	17
2.4	Viscosity as a function of shear rate in Al ₂ O ₃ - water based nanofluids at the volume concentration from 1 to 5% (after 2weeks)	17
2.5	Viscosity as a function of shear rate for Al ₂ O ₃ - water based nanofluids at the volume concentrations from 1 to 5% (after re- ultrasonication)	18
2.6	Relative viscosity of Al ₂ O ₃ - water based nanofluids as a function of volumetric concentration	21
3.1	Comparison of SEM and TEM	22
3.2	X-ray diffraction by crystal	23
3.3	X-ray diffraction for finding interplanar distances	24
3.4	Oscar ultrasonicator	24
3.5	Cone and plate type Brookfield LVDV-III-Pro viscometer	26
4.1	TEM image of Al ₂ O ₃ nanoparticles	30
4.2	XRD pattern image	31
4.3	Image of the prepared Al ₂ O ₃ - (EG) based nanofluids of different volumetric concentrations	33
4.4	Shear stress versus shear rate of pure EG (0% Al ₂ O ₃ concentration)	33

4.5	Shear stress versus shear rate of Al ₂ O ₃ - EG based nanofluid at a volumetric concentration of 0.005%	34
4.6	Shear stress versus shear rate of Al ₂ O ₃ - EG based nanofluid at a volumetric concentration of 0.01%	34
4.7	Shear stress versus shear rate of Al ₂ O ₃ - EG based nanofluid at a volumetric concentration of 0.05%	35
4.8	Shear stress versus shear rate of Al ₂ O ₃ - EG based nanofluid at a volumetric concentration of 0.1%	35
4.9	Viscosity versus shear rate of pure EG (0% Al ₂ O ₃ concentration)	36
4.10	Viscosity versus shear rate of Al ₂ O ₃ - EG based nanofluid at a volumetric concentration of 0.005%	37
4.11	Viscosity versus shear rate of Al ₂ O ₃ - EG based nanofluid at a volumetric concentration of 0.01%	37
4.12	Viscosity versus shear rate of Al ₂ O ₃ - EG based nanofluid at a volumetric concentration of 0.05%	38
4.13	Viscosity versus shear rate of Al ₂ O ₃ - EG based nanofluid at a volumetric concentration of 0.1%	38
4.14	Viscosity versus temperature of Al ₂ O ₃ - EG based nanofluids at different volumetric concentrations (at a constant shear rate of 114 /s)	39
4.15	Relative viscosity versus volumetric concentration of Al ₂ O ₃ - EG based nanofluids (at a constant shear rate of 114 /s and a constant temperature of 25 °C) and its comparison with the theoretical models	40
4.16	Image of the prepared Al ₂ O ₃ - (EG + H ₂ O) based nanofluids of different volumetric concentrations	41
4.17	Shear stress versus shear rate of pure (EG + H ₂ O) (0% Al ₂ O ₃ concentration)	42
4.18	Shear stress versus shear rate of Al ₂ O ₃ - (EG + H ₂ O) based nanofluid at a volumetric concentration of 0.005%	42
4.19	Shear stress versus shear rate of Al ₂ O ₃ - (EG + H ₂ O) based nanofluid at a volumetric concentration of 0.01%	43
4.20	Shear stress versus shear rate of Al ₂ O ₃ - (EG + H ₂ O) based nanofluid at a	43

	volumetric concentration of 0.05%	
4.21	Shear stress versus shear rate of Al ₂ O ₃ - (EG + H ₂ O) based nanofluid at a volumetric concentration of 0.1%	44
4.22	Viscosity versus shear rate of pure - (EG + H ₂ O)	45
4.23	Viscosity versus shear rate of Al ₂ O ₃ - (EG + H ₂ O) based nanofluid at a volumetric concentration of 0.005%	45
4.24	Viscosity versus shear rate of Al ₂ O ₃ - (EG + H ₂ O) based nanofluid at a volumetric concentration of 0.01%	46
4.25	Viscosity versus shear rate of Al ₂ O ₃ - (EG + H ₂ O) based nanofluid at a volumetric concentration of 0.05%	46
4.26	Viscosity versus shear rate of Al ₂ O ₃ - (EG + H ₂ O) based nanofluid at a volumetric concentration of 0.1%	47
4.27	Viscosity versus temperature of Al ₂ O ₃ - (EG + H ₂ O) based nanofluids at different volumetric concentrations (at a constant shear rate of 114 /s)	48
4.28	Relative viscosity versus volumetric concentration of Al ₂ O ₃ - (EG + H ₂ O) based nanofluids (at a constant shear rate of 114 /s and constant temperature of 25 °C) and its comparison with the theoretical models	49
4.29	Shear stress versus shear rate at constant temperature of 25 °C for Al ₂ O ₃ concentration of 0.01 % in (EG) and (EG + H ₂ O) as base fluid	50
4.30	Viscosity versus shear rate of (EG) and (EG + H ₂ O) based nanofluids (at a constant temperature of 25 °C and a constant Al ₂ O ₃ concentration of 0.01 %)	51
4.31	Viscosity versus temperature of (EG) and (EG + H ₂ O) based nanofluids (at a constant Al ₂ O ₃ concentration of 0.01 % and a constant shear rate of 114 (1/s)	52
4.32	Relative viscosity versus concentration of (EG) and (EG + H ₂ O) based nanofluids (at a constant temperature of 25 °C and a constant shear rate of 114 (1/s)	53

LIST OF TABLES

No.	DESCRIPTION	Page
1.1	Comparison of microparticles and nanoparticles	2
4.1	Constants and variables in the experiment	29
4.2	Physical properties of alumina nanoparticles	30
4.3	Peak list of the XRD pattern image	31
4.4	Volumetric Concentrations of Al ₂ O ₃ Nanoparticles with the corresponding mass	32
A.1	Experimental data of ethylene glycol at different temperatures and shear rates	59
A.2	Experimental data of Al ₂ O ₃ - ethylene glycol based nanofluid at a volumetric concentration of 0.005% at different temperatures and shear rates	60
A.3	Experimental data of Al ₂ O ₃ - ethylene glycol based nanofluid at a volumetric concentration of 0.01% at different temperatures and shear rates	61
A.4	Experimental data of Al ₂ O ₃ - ethylene glycol based nanofluid at a volumetric concentration of 0.05% at different temperatures and shear rate	62
A.5	Experimental data of Al ₂ O ₃ - ethylene glycol based nanofluid at a volumetric concentration of 0.1% at different temperatures and shear rates	63
A.6	Experimental data of EG and H ₂ O mixture in 60:40 ratio by volume at different temperatures and shear rates	64
A.7	Experimental data of Al ₂ O ₃ - (EG and H ₂ O mixture) based nanofluid at a volumetric concentration of 0.005% at different temperatures and shear rates	65
A.8	Experimental data of Al ₂ O ₃ - (EG and H ₂ O mixture) based nanofluid at a volumetric concentration of 0.01% at different temperatures and shear rates	66
A.9	Experimental data of Al ₂ O ₃ - (EG and H ₂ O mixture) based nanofluid at a volumetric concentration of 0.05% at different temperatures and shear rates	67
A.10	Experimental data of Al ₂ O ₃ - (EG and H ₂ O mixture) based nanofluid at a volumetric concentration of 0.1% at different temperatures and shear rates	68

ACRONYMES

DI	Deionized Water
DW	Distilled Water
nm	Nanometer
SEM	Scanning Electron Microscope
TEM	Transmission Electron Microscope
XRD	X- Ray Diffraction
EG	Ethylene Glycol
H₂O	Water
Al₂O₃	Aluminum Oxide
cP	Centi Poise
cSt	Centi Stoke

INTRODUCTION

Historically, thermal transport properties of colloidal systems have been of little interest to the scientific world. Due to recent advancements in nanoparticle colloid production, such fluids are being explored for their uses like heat transfer. This leads to the creation of nanoparticle colloids with the ability to remain in dispersion indefinitely. The aim of this study is to understand the factors affecting the viscosity of nanofluids.

1.1 Nanofluids

Nanofluids (nanoparticle, fluid suspensions) is the term developed by Choi [1] to describe the new class of nanotechnology based heat transfer fluids that exhibit thermal properties superior to those of their host fluids or conventional particle fluid suspensions. Nanofluids are suspension of metallic or metal-oxide solid nano particles with size varying generally from 1 to 100 nm, dispersed in conventional liquids such as water, ethylene glycol and engine oils etc. Nanofluid is a new, innovative class of heat transfer fluids represents a rapidly emerging field where nano science and thermal engineering coexist. Nanofluids have unique features different from conventional solid liquid mixtures in which mm or μm sized particles of metals and non metals are dispersed. Due to their excellent characteristics, nanofluids find wide applications in the area of heat transfer technology.

1.2 Importance of Nanofluids

Numerous theoretical and experimental studies of suspensions containing solid particles have been conducted since Maxwell's theoretical work was published more than 100 years ago. However, due to the large size and high density of the micro particles, there is no good way to prevent the solid particles from settling out of suspension. The lack of stability of such suspensions induces additional flow resistance and possible erosion. Table 1.1 shows the comparison of microparticles and nanoparticles.

The importance of Nanofluids is summarized below:

- Nanofluids can be considered to be the next-generation heat transfer fluids as they offer exciting new possibilities to enhance heat transfer performance compared to pure liquids.

- They have superior properties compared to conventional heat transfer fluids, as well as fluids containing micro-sized metallic particles.
- The much larger relative surface area of nanoparticles, compared to those of conventional particles, should not only significantly improve heat transfer capabilities, but also should increase the stability of the suspensions.
- Also, nanofluids can improve abrasion-related properties as compared to the conventional solid/fluid mixtures.
- Successful employment of nanofluids will support the current trend toward component miniaturization by enabling the design of smaller and lighter heat exchanger systems.
- This is of major importance for electronics and microelectronics where liquids cooling systems are necessary and miniaturizing is needed.

	Microparticles	Nanoparticles
Stability	Settle	Stable (remain in suspension almost indefinitely)
Surface/volume ratio	1	1000 times larger than that of microparticles
Conductivity ^a	Low	High
Clog to microchannel	Yes	No
Erosion	Yes	No
Pumping Power	Large	Small
Nanoscale Phenomena	No	Yes

^a At the same volume fraction.

Table 1.1 Comparison of microparticles and nanoparticles [2]

1.3 Preparation of Nanofluids

Here, we briefly mention the techniques that, so far, have been most commonly used. There are mainly two techniques used to produce the nanofluids: the two-step and the single-step process.

1.3.1 Two - step process

Several studies, including the earliest investigations of nanofluids, used a two-step process.

1. The nanoparticles or nanotubes are first produced as a dry powder, often by inert gas condensation.
2. The nanoparticles or nanotubes are then dispersed into a fluid in a second processing step. Simple techniques such as ultrasonic agitation or the addition of surfactants to the fluids are sometimes used to minimize particle aggregation and improve dispersion behavior.

Research on this method provided the following data:

- Such a two-step process works well in some cases, such as nanofluids consisting of oxide nanoparticles dispersed in deionized water.
- Less success has been found when producing nanofluids containing heavier metallic nanoparticles.
- Since nanopowder synthesis techniques have already been scaled up to industrial production levels by several companies, there are potential economic advantages in using two-step synthesis methods that rely on the use of such powders.
- For example, Eastman et al. [3], Lee et al. [4], and Wang et al. [5] used this method to produce Al_2O_3 nanofluids. Also, Murshed et al. [6] prepared TiO_2 suspension in water using the two-step method.

1.3.2 Single - step process

Single-step nanofluid processing methods have also been developed.

- Nanofluids containing dispersed metal nanoparticles have been produced by a ‘direct evaporation’ technique [7]. As with the inert gas condensation technique, this involves the vaporization of a source material under vacuum conditions.
- An advantage of this technique is that nanoparticle agglomeration is minimized.
- While a disadvantage is that only low vapor pressure fluids are compatible with the process.
- Various single-step chemical synthesis techniques can also be employed to produce nanofluids. For example, Zhu et al. [8] presented a novel one-step chemical method for preparing copper nanofluids.

1.4 Materials for Nanofluids

Nanofluids are made of nanometer sized substances engineered on the atomic or molecular scale to produce either new or enhanced physical properties, which are not exhibited by conventional bulk solids.

- **Nanoparticle material types:** Nanoparticles used in nanofluids have been made of various materials, such as nitride ceramics (AlN, SiN), carbide ceramics (SiC, TiC), metals (Cu, Ag, and Au), oxide ceramics (Al₂O₃, CuO), semiconductors (TiO₂, SiC), carbon nanotubes and composite materials such as alloyed nanoparticles Al₇₀Cu₃₀.
- **Host liquid types.** Many types of liquids, such as water, ethylene glycol and oil have been used as host liquids in nanofluids.

1.5 Viscosity of Nanofluids

1.5.1 Viscosity

Informally, viscosity is the quantity that describes a fluid's resistance to flow. Fluids resist the relative motion of immersed objects through them as well as to the motion of layers with differing velocities within them. Formally, viscosity is the ratio of the shearing stress ($\tau = F/A$) to the velocity gradient (du/dy) in a fluid.

$$\mu = \frac{\tau}{\left(\frac{du}{dy}\right)}$$

The SI unit of viscosity is the pascal second [Pa s], which has no special name. The pascal second is rarely used in scientific and technical publications today. The most common unit of viscosity is the dyne second per square centimeter [dyne s/cm²], which is given the name poise [P].

$$1 \text{ pascal second} = 10 \text{ poise}$$

There are actually two quantities that are called viscosity. The quantity defined above is sometimes called **dynamic viscosity**, absolute viscosity, or simple viscosity to distinguish it from the other quantity, but is usually just called viscosity. The other quantity called kinematic viscosity (represented by the symbol ν "nu") is the ratio of the viscosity of a fluid to its density.

$$\nu = \frac{\eta}{\rho}$$

Kinematic viscosity is a measure of the resistive flow of a fluid under the influence of gravity. The SI unit of kinematic viscosity is the square meter per second [m²/s], which has no special name. This unit is so large that it is rarely used. A more common unit of kinematic viscosity is the square centimeter per second [cm²/s], which is given the name stokes [St]. Even this unit is also a bit too large and so the most common unit is probably the square millimeter per second [mm²/s] or centistokes [cSt].

1.5.2 Newtonian behavior

The Newton's law of viscosity is given below:

$$\tau = \mu \left(\frac{du}{dy} \right)$$

τ is the shear stress applied,

μ is the dynamic viscosity of the fluid,

$\left(\frac{du}{dy} \right)$ is the shear strain rate.

The fluids which obey this Newton's law of viscosity are known as the Newtonian Fluids. Therefore, for the Newtonian fluids, the viscosity value do not change by the change in the Shear strain rate i.e. it remains constant. And, the shear stress is directly proportional to the shear strain. The fluids which do not obey this Newton's law of viscosity are known as the Non Newtonian Fluids. And, the Non- Newtonian fluids show two types of behaviors:

Shear thinning behavior: The fluids whose viscosity value decreases with an increase in the shear rate are said to have shear thinning behavior.

Shear thickening behavior: The fluids whose viscosity value increases with an increase in the shear rate are said to have shear thickening behavior.

1.6 Factors Effecting the Viscosity of Nanofluids

The viscosity of nanofluids is effected by many factors such as

- Concentration.
- Temperature.
- Shape of nanoparticles.
- Size of nanoparticles.
- Base fluid used.
- Surfactants used.
- pH value.
- Sonication time.

The effect of all these factors will now be discussed in the following pages.

1.6.1 Effect of nanoparticles used

As the nanofluid is composed of two main components, the nanoparticles and the base fluid used and, the colloidal stability of the nanofluid is one of the major factor that influences the viscosity of the nanofluids. Therefore, it becomes necessary to understand the colloidal stability so as to draw the correct conclusions of the factors influencing the viscosity of nanofluids. The basics of the colloidal stability have been discussed below. One can consider that the particles have multiple attractive and repulsive forces. These forces are a function of the separation distance between the particles. A summation of the

forces would give a total interaction potential curve as shown in the following figure drawn between free energy and interparticle distance r .

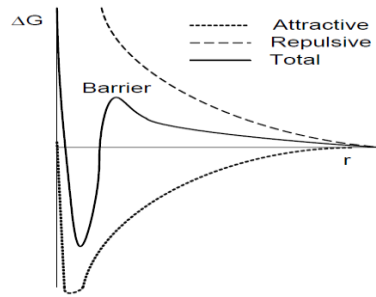


Figure 1.1 Interaction potential energy curve

The creation of a local maximum in this curve would amount to a barrier. Therefore, the colloidal stability is achieved through the creation of this energy barrier which would prevent the particles from coming in close proximity and thus aggregating. The height of the energy barrier should be somewhat greater than $k_B T$ the thermal energy of the liquid, where k_B is the Boltzmann constant. This thermal energy of the liquid is what creates the Brownian motion. Brownian motion is the only force which can push the particle together over the energy barrier. Due to the probabilistic nature of Brownian motion, usually a barrier of $10k_B T$ is required to assure good stability. Barrier height is dependent on fluid and particle composition, temperature, and pressure. As can be seen, the particles possess greater energy to overcome this barrier at higher temperatures, and the colloidal system aggregates beyond a critical value called the critical flocculation temperature. Therefore, as discussed above, the stability of the colloidal system depends on the energy barrier and this energy barrier keeps the system well dispersed and prevents coagulation. This barrier height is dependent on the fluid and particle composition. Therefore, the size of the particles as well their chemical composition and their structures determines the stability of the nanofluid system. And, the stability in turn affects the viscosity of the nanofluids. The effect of nanoparticles size, composition of nanoparticles on the viscosity, as found in the different research papers is discussed in the Literature Review.

1.6.2 Effect of sonication time

The small particle size dramatically increases the surface to volume ratio of the system. In order to increase the surface area of a material energy must be given to the system. This energy is input by breaking and dispersing the particles. Standard methods for breaking and dispersing are high speed stirring, ball milling, ultrasonication and high shear nozzles.

Therefore the distance from the point of energy stability is increased by increasing the surface area of the particles with these methods.

Sonication: High-frequency sound waves typically used to agitate particles in a sample. Therefore, it is usually done for the dispersion of nanoparticles in a liquid. In the laboratory, it is usually applied by a device known as a sonicator. Sonication can be used to speed dissolution, by breaking intermolecular interactions. Sonication is commonly used in nanotechnology for evenly dispersing nanoparticles in liquids. It is mainly useful when it is not possible to stir the sample. Therefore, as the sonication time is increased the dispersion of the nano particles increases which increases the stability. And discussed earlier stability affects the viscosity of the nanofluids therefore we can say that the sonication time has an effect on the viscosity of nanofluids.

1.6.3 Effect of base fluid & surfactants

It has been found that, the effect of base fluid on the viscosity of nanofluids has come from the stability of the nanofluids. Therefore, as discussed above, the stability of the colloidal system depends on the energy barrier and the barrier height is dependent on the fluid and particle composition. Therefore, the chemical composition of base fluids determines the stability of the nanofluid system and, the stability in turn affects the viscosity of the nanofluids. There are several methods for the creation of the energy barrier that exist to keep the nanofluid system stable. If the additional electrostatic or steric energies are designed properly one can create an energy barrier which makes stable nanofluids. Two major methods will be discussed here: surface charging and surfactant adsorption.

Surface charging: It is typically achieved with the electrical double layer. The simplest way to visualize the double layer is as an ionic atmosphere around the particle which is created by the chemical reaction between the solvent and the particle. The surface of the particle will react with the solvent to create charged groups on the surface. This in turn builds the atmosphere of oppositely charged ions to balance the overall charge.

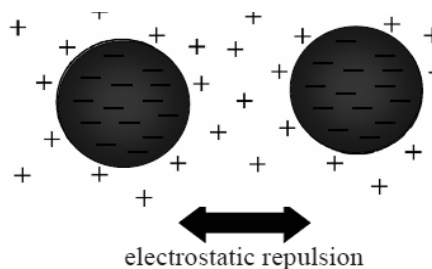


Figure 1.2 Surface charging of nanoparticles

The size and charge concentration of the double layer, which is dependent on the composition of the solvent, directly affect the stability of colloids. The creation of like charges on the surfaces of the particles makes a strong repulsive force between particles which falls off exponentially as the interparticle distance is increased. This force is seen as the barrier in the total interaction potential. At long distances the double layer covered particle would be seen as neutral.

Surfactant adsorption: The second method of colloid stabilization is the adsorption of surfactants or steric repulsion. Surfactants are wetting agents that lower the surface tension of a liquid, allowing easier spreading, and lower the interfacial tension between two liquids. They can be seen simply as string-like materials with hydrophobic heads and hydrophilic tails. The concept is similar to the double layer, except that the surfactants are anchored to the surface and the tails of the surfactants reach out into the fluid. The tails prevent the particles from approaching each other close enough to agglomerate.

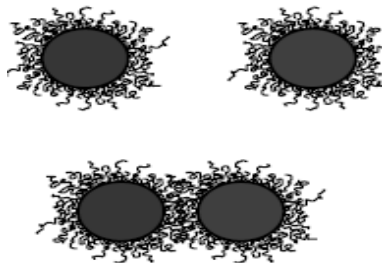


Figure 1.3 Steric repulsions caused by the surfactants

Steric repulsion allows for more stability of a colloid under variable pH or concentration conditions. The amount of adsorption determines the stability of the resultant colloid. It is therefore very important to select the proper surfactant for the particular fluid/particle combination which often times requires trial and error. The works of Krishnakumar [9] showed that Aerosol-OT (AOT) can effectively help to stabilize dispersions of alumina in non-polar solvents, where surface charge stabilization is not possible.

1.6.4 Effect of pH value

Basically, pH is the measurement of the hydrogen ion concentration, $[H^+]$. It is defined as the negative logarithm of the hydrogen ion concentration as:

$$pH = -\log [H^+]$$

$[H^+]$ is hydrogen ion concentration in mol/L.

The pH unit measures the degree of acidity or basicity of a solution. The pH value is an expression of the ratio of $[H^+]$ to $[OH^-]$ (hydroxide ion concentration). Hence, if the $[H^+]$ is greater than $[OH^-]$, the solution is acidic. Conversely, if the $[OH^-]$ is greater than the

[H⁺], the solution is basic. This value ranges from 0 to 14 pH. Values below 7 pH exhibit acidic properties. Values above 7 pH exhibit basic (also known as caustic or alkaline) properties. At 7 pH value, the ratio of [H⁺] to [OH⁻] is equal and, therefore, the solution is neutral. Due to the high surface energy of nanoparticles, it is easy for nanoparticles to coagulate and difficult to disperse in the base fluid. This leads to changes of the morphology and of volume fraction resulting in low fluidity. Therefore, controlling the coagulation of nanoparticles in the nanofluid becomes the primary issue. The pH value of nanofluids such as Al₂O₃ - H₂O is controlled using hydrochloric acid (HCl) and sodium hydroxide (NaOH). Well-dispersed suspension can be obtained with high surface charge density to generate strong repulsive forces. Changing suspension pH value generates strong repulsive forces and reduces the coagulation of nanoparticles to obtain a low viscosity (well-dispersed) suspension. Therefore, an optimum value of pH can result in the lowest viscosity. Thus, adjusting the nanofluid pH value is recommended to improve the dispersive stability and hence lowest viscosity. It has been found that the pH value should be far from the isoelectric point of nanoparticles. This ensures the nanoparticles are well dispersed and the nanofluid is stable because of very large repulsive forces among the nanoparticles. For example, The pH of the prepared Al₂O₃ nanofluids were measured to be around 5 which is far from the isoelectric point of 9.2 for alumina nanoparticles therefore the nanofluid was assumed to be stable [10].

1.6.5 Effect of concentration

The viscosity of nanofluids also depends strongly on the volumetric concentrations of the nano particles in the base fluid. The viscosity increases with an increase in volumetric concentrations of the nano particles in the base fluid. But the increase is non- linear and different for different types of fluids. With an increase in the nanoparticle volumetric concentrations, the more number of the nanoparticles comes into contact with the base fluid. Therefore, with the increased number of particles in contact, the total surface area in contact with the base fluid increases. The increased contact surface area causes more resistance to the movement of the base fluid molecules, thereby increasing the viscosity of the nanofluid.

1.6.6 Effect of temperature

The increase in temperature has shown to decrease the viscosities for all nanofluids, which can be attributed to the decrease in inter-particle and inter-molecular adhesive forces. This

is due to the thermal degradation of the basefluid at higher temperatures and also due to the agglomeration or clinging of the nanoparticles with each other at higher temperatures. The agglomeration decreases the surface area in contact with the base fluid at any concentration and the decreased contact surface area reduces the viscosity. An interesting observation during viscosity measurements at higher temperatures is the hysteresis behavior in nanofluids. It is observed that certain critical temperature exists, beyond which, on cooling down the nanofluid from a heated condition, it do not traces the same viscosity curve corresponding to the heating part of the cycle.

1.7 Objectives

- To prepare the Al_2O_3 based Nanofluids.
- To characterize the nanomaterial used.
- To investigate the various factors effecting the viscous behavior of Al_2O_3 nanoparticles in two base fluids- (Ethylene Glycol) and (a mixture of Water and Ethylene Glycol mixed in the ratio of 60:40 by volume) such as, volumetric concentration of the nanoparticles, temperature, shear rate.
- To study the rheological behavior i.e. Newtonian/ Non- Newtonian behavior.

LITERATURE REVIEW

This chapter reviews the previous published literature on nanofluids. This will provide a better understanding about the topic and will lay the foundation for the further work which is to be carried out. The literature review on the viscous behavior of different nanofluids is given below.

2.1 Viscous Behavior of Different Nanofluids

Namburu *et al.* [11] investigated the viscosity of silicon dioxide (SiO_2) nanoparticles with various diameters (20, 50 and 100 nm) suspended in a 60:40 ratio of ethylene glycol and water mixture. Nanofluids with particle volume percentages ranging from 0 to 10 % were examined. Viscosity experiments were carried out over wide temperature ranges, from -35 to 50 $^{\circ}\text{C}$, to demonstrate their applicability in cold regions. Namburu showed that, for temperatures greater than -10 $^{\circ}\text{C}$, silicon dioxide nanofluids display Newtonian behavior. For the temperatures below -10 $^{\circ}\text{C}$, the nanofluids demonstrate non-Newtonian behavior. The viscosity diminishes exponentially as the sample fluid temperature increases. Furthermore, it was shown that with higher nanoparticle concentrations, nanofluids possess higher viscosity. The shape of each curve for different concentrations of nanofluids was similar, which indicated the consistency of trend of the experimental measurements. Similar trends were observed for viscosity measurements of silicon dioxide nanofluids with nanoparticle diameters of 20 and 100 nm. It was shown that DVI (degree of viscosity increase) reduces from -35 to 50 $^{\circ}\text{C}$, for all nanofluid concentrations. If the concentration of nanoparticles was low, the DVI was low as well. It was inferred that for the same volumetric concentration of 8 %, silicon dioxide nanofluids with highest nanoparticle diameter 100 nm have the lowest viscosity. Similar trends of experimental results were obtained for all concentrations of silicon dioxide nanofluids.

Chen *et al.* [12] studied the viscosity of ethylene glycol based nanofluids containing titanate nanotubes over $20 - 60$ $^{\circ}\text{C}$ and a particle concentration of 0 - 8 % (mass). It was observed that the EG - TNT nanofluids exhibit highly shear-thinning behavior (Non Newtonian) particularly when the TNT concentration exceeds 2 %. The temperature had a very strong effect on the rheological behavior of nanofluids with higher temperatures giving stronger shear thinning. For shear rates below 10 s^{-1} value, the shear viscosity was

found to be increased with increased temperature, whereas the trend was reversed when the shear rate was above 10 s^{-1} value. It was also shown that the strongest shear thinning occurs at $40 - 60 \text{ }^{\circ}\text{C}$, whereas very weak-shear thinning takes places at $20 - 30 \text{ }^{\circ}\text{C}$. It was also noted that the shear viscosity of nanofluids at all temperatures investigated approaches a constant at high-shear rates.

Guo *et al.* [13] studied the viscosity of a spherical-shaped $\gamma - \text{Fe}_2\text{O}_3$ nanoparticles with diameter of 20 nm dissolved in the mixture of ethylene glycol and deionized water with a volume ratio of 45:55 as a base fluid and surfactant used was sodium oleate. It was observed that the viscosity of the nanofluids increases with an increase in the volume fraction, but decreases with an increase in the temperature. The behavior of these nanofluids was close to the typical Newtonian fluids. And it was also found that the experiment data for viscosity of the nanofluids was much larger than the data predicted by using theoretical models.

Xinfang *et al.* [14] performed experimental investigations on the viscosity of Cu - H_2O Nanofluids. The mass fractions of copper nanoparticles in the experiment were varied between 0.04 % and 0.16 % with the temperature range of $30 - 70 \text{ }^{\circ}\text{C}$. An anionic surfactant, sodium dodecyl benzene sulfonate (referred to as SDBS) was used for the dispersion of copper nanoparticles. The viscosity of SDBS solution was found to decrease with an increase in temperature. The higher the mass fraction of SDBS solution was, the bigger the apparent viscosity was. It was observed that the apparent viscosity of 0.04 % copper nano - suspensions was very close to the viscosity of 0.04 % dispersant solution. The experimental results showed that the apparent viscosity of the copper nano-suspensions decreases with the temperature increase, and increases slightly with increasing the mass fraction of SDBS dispersant, and almost remains invariable with an increase in the mass fraction of Cu. So, the temperature and SDBS concentration are the major factors affecting the viscosity of the nanoparticle suspensions. It has been also found that, as the dispersant concentration increases, the apparent viscosity of copper nano-suspension also increased, with a maximal value at the 0.12 % SDBS, then the viscosity remained almost constant, which indicates the influence of SDBS concentration on the viscosity of nano-suspension exists an optimizing value. So at the 0.12 % SDBS, the system is more stable, which suggests SDBS dispersant yields well dispersed system.

Kole *et al.* [15] investigated the viscosity of the stable nanofluids, prepared by dispersing 40 nm diameter spherical CuO nanoparticles in gear oil. The surfactant used was oleic acid. Over the measured temperature range viscosity of the oil was found to be independent of the shear strain rate, indicating Newtonian behavior. It was also confirmed that the addition of a small quantity of surfactant do not change the absolute value of base fluid viscosity and its Newtonian characteristics. However, as the CuO loading in gear oil was increased, non-Newtonian characteristics of the fluid becomes evident. At lower particle volume fraction of CuO (viz.0.005), the shear stress was found to increase linearly with the shear strain rate. However, for higher CuO volume fractions greater than 0.005, shear stress was found to vary nonlinearly with shear strain rate, indicating the onset of shear thinning behavior and was consistent with the observed decrease in viscosity with increasing shear strain rate. Relative viscosity of CuO nanofluids increased with the increased nanoparticle concentration. Viscosity of the nanofluid enhanced nearly by three times than that of gear oil, as CuO volume fraction loading increased to 0.025. This was consistent with the fact that increase in nanoparticle concentration in nanofluid increases the fluid's internal shear stress, hence the viscosity. It was also observed that the viscosity of the nanofluid decreases with the rise in temperature.

Phuoc *et al.* [16] studied the viscosity of Fe₂O₃ - deionized water nanofluids containing 0.2 % polymer by weight as a dispersant. Two polymers were used: Poly Vinyl Pyrrolidone (PVP) and Poly Ethylene Oxide (PEO) were used as surfactants. It was observed that a nanofluid prepared with Fe₂O₃ nanoparticles in DW - 0.2 % PVP behaved as a Newtonian fluid when the volume fraction was less than 0.02. For the volume fraction more than 0.02 the suspension became non-Newtonian with shear-thinning behavior. The viscosity was found to increase with an increase in particle volume fraction and it decreased significantly towards that of the base fluid viscosity as the shear rate was increased. Similar results were also observed when DW - 0.2 % PEO was used as the base fluid. The suspension, however, switched to its non-Newtonian and shear-thinning behavior at volume fraction as low as 0.02. And, it was also found that for any given shear rates, the measured viscosity increased exponentially with the particle volume fraction.

Duangthongsuk *et al.* [17] studied TiO₂ nanoparticles dispersed in water with volume concentration of 0.2 - 2 %. The data was collected for temperatures ranging from 15 °C to 35°C. The viscosity of the nanofluids was found to increase with the decrease in nanofluid

temperature and with the increase in particles volumetric concentration. It was found that the viscosity of these nanofluids was higher than the base fluid by about 4 - 15%.

Garg *et al.* [18] investigated the effect of sonication on the viscosity of multi-wall carbon nanotube (MWCNT) - based aqueous nanofluids. De - ionized (DI) water was used as the base fluid and the surfactant used was Gum Arabic (GA). All the four samples studied were constituted of MWCNT (1 % by mass) and GA (0.25 % by mass), but sonicated for different amount of times as given below:

Sample A: sonicated for 20 min.

Sample C: sonicated for 60 min.

Sample B: sonicated for 40 min.

Sample D: sonicated for 80 min.

It was observed that, the MWCNT aqueous nanofluids displayed a non-Newtonian behavior especially at 15 °C. A shear thinning behavior was observed resulting in a decrease in viscosity with an increase in shear rate up to 60 s⁻¹ value. In case of 0.25 wt% GA aqueous solution, shear thinning was observed initially (up to 60 s⁻¹) but a slight shear thickening can be observed at 75 s⁻¹ value. A shear thinning effect was explained by possible de-agglomeration of bundled nanotubes or realignment in the direction of the shearing force, resulting in less viscous drag. A slight shear thickening was attributed to the unique fluid properties. The viscosity of the nanotube suspension first increased from sample A to sample B, and thereafter decreased with an increase in sonication time. After 40 min of sonication, it was found that the viscosity continuously decreased with further sonication. The optimum sonication time was found to be 40 min at 1 % (mass) MWCNT concentration.

Abareshi *et al.* [19] investigated α -Fe₂O₃ nanoparticles dispersed in glycerol as the base fluid. The viscosity of nanofluids was found to decrease with the increase in the shear rate and hence the nanofluids considered were non-Newtonian fluids with shear-thinning behavior. At lower temperatures, the shear-thinning behavior was more obvious. The measured viscosity of nanofluids was found to decrease with the increase in fluid temperature. The viscosity of the nanofluids increased with the increase in volume fraction. The non-Newtonian character of the nanofluids was more obvious for higher volume fractions where the amount of aggregation was higher. And, the comparison of measured viscosity values with the predicted values from the models was also shown. It was found that the measured viscosity of nanofluids was much higher than those of predicted values using the Einstein, Brinkman, and Batchelor models.

Wei et al. [20] investigated the viscosity of ethylene glycol based ZnO nanofluid. Viscosity of the ZnO (at $\leq 2\%$ by volume) - EG based nanofluid was found to be independent of the shear rate varied in the range of 20 to 100 s^{-1} and a temperature range of 20 - 60 $^{\circ}C$. Therefore, the ZnO nanoparticles (at $\phi \leq 2\%$ by volume) behaved as a Newtonian fluid. While for the ZnO - EG nanofluid with $\phi \geq 0.03$, the shear-shinning behavior was observed. For higher volume concentrations and lower temperatures, the shear-shinning behavior was more obvious.

Namburu et al. [21] investigated the copper oxide nanoparticles with an average diameter of 29 nm. Nanoparticles with different volumetric concentrations (1%, 2%, 3%, 4%, 5 % and 6.12%) were dispersed in 60:40 ratios of ethylene glycol and water mixture as the base fluid. It was observed that viscosity decreased exponentially with the increase in fluid temperature. Higher concentrations of nanofluids possess higher viscosity. It was also found that the relative viscosity diminishes as temperature increases, at a higher rate for higher concentrations of nanoparticles. At lower concentrations, the change in relative viscosity over temperature was minimal.

2.2 Factors Effecting Viscosity

The main parameters which effect the viscous behavior of $Al_2O_3 - H_2O$ based nanofluids are nanoparticles size, volume concentration, temperature and pH value of the nanofluid.

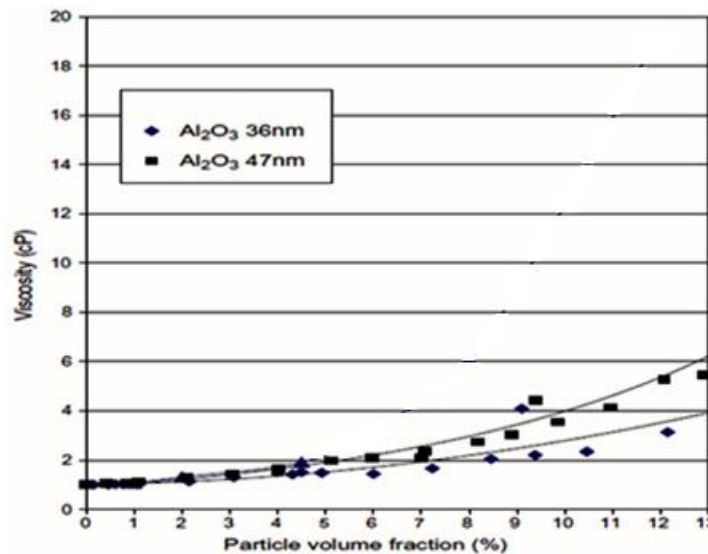


Figure 2.1 Effect of nanoparticles size on the viscosity of $Al_2O_3 - H_2O$ based nanofluids [22]

Reported work in figure 2.1 shows that viscosity of Al_2O_3 - H_2O based nanofluids with 36 nm particle-size are clearly lower than those with 47 nm particles. This emphasizes the effect of size of nanoparticles on the viscosity. Such differences become more pronounced for particle volume fractions higher than 5%. Therefore, it can be understood that the viscosity of the nanofluids decreases with the decrease in the Nanoparticles size. Hence, the size of the nanoparticles is very important in order to study of viscous behavior of nanofluid.

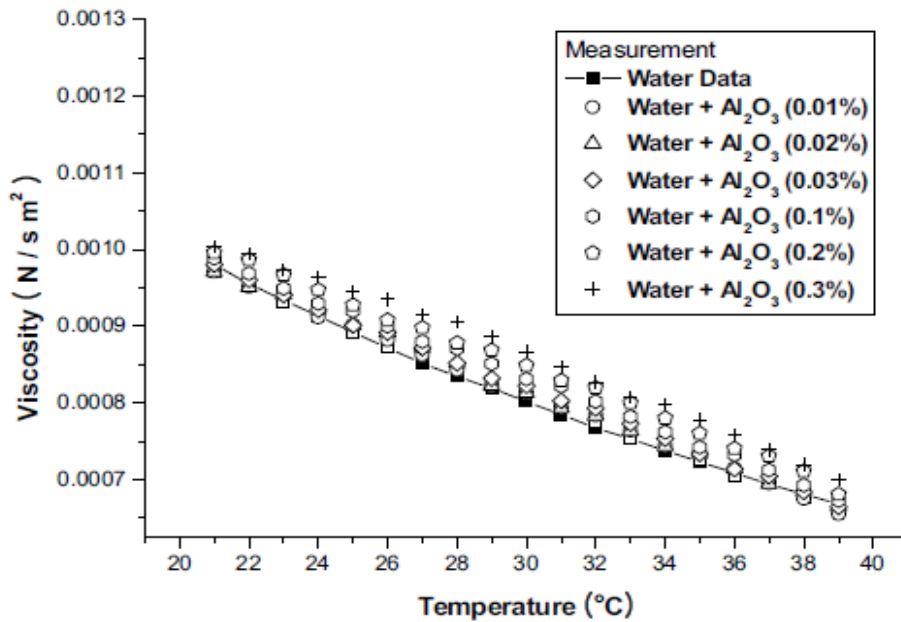


Figure 2.2 Variation of effective viscosity of Al_2O_3 - water nanofluids with temperature at different nanoparticle volume fractions [23]

Figure 2.2 shows the variation in the nanofluids viscosity for the Al_2O_3 - H_2O based nanofluids for different volume concentration (0.01 % to 0.03 %) and for the temperature range from 21 °C to 39 °C. It can be seen from figure 2.2, that at any temperature, the viscosity increases with an increase in concentrations. And, at any concentration, the viscosity of the nanofluid decreases almost linearly with an increase in the temperature, which can be attributed to the decrease in inter-particle and inter-molecular adhesive forces which ultimately decrease the viscosity of the nanofluid. The pH value of the nanofluids also plays a very important role to evaluate their performance. Basically pH value decides whether solution is stable or not, if solution is stable enough then it will exhibit very good thermal properties, otherwise not.

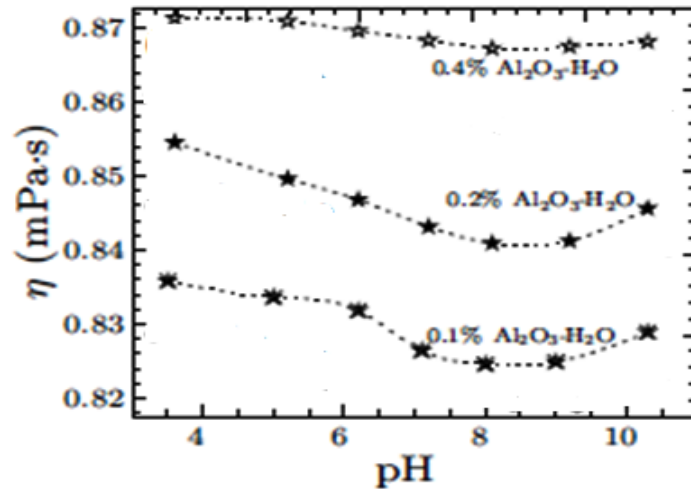


Figure 2.3 Variation of the viscosity with pH of the Al₂O₃ -H₂O nanofluid [24]

Figure 2.3 shows how viscosity varies with pH value of the solution. It can be seen from figure 2.3, that there exists an optimum value of pH, at which the viscosity is minimum for each concentration. Above and below this optimum pH value the viscosity increases. And, the value of this optimum pH increases with an increase in the concentration of nanoparticles. Changing suspension pH value, changes the net charge on the particles. The higher charge on the particles generates strong repulsive forces and reduces the aggregation of the nanoparticles. The pH value at which net charge on the particles on the particles is zero is known as the isoelectric point. At isoelectric point particles have maximum chances to agglomerate and solution will be least stable.

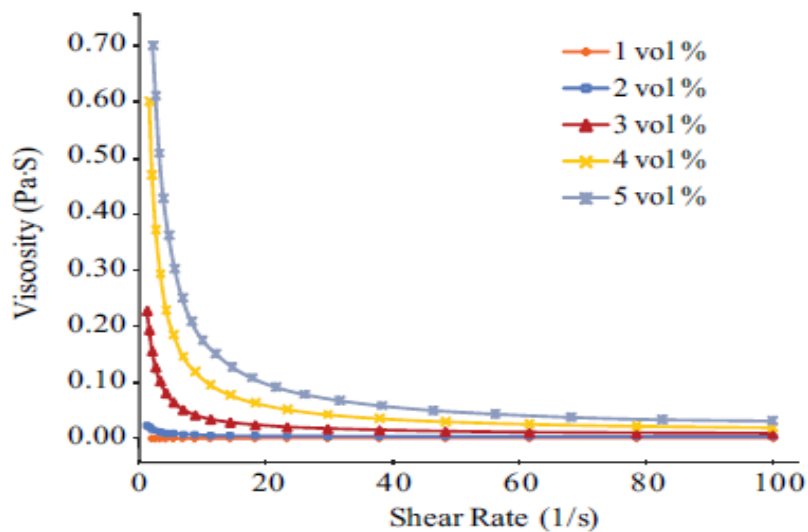


Figure 2.4 Viscosity as a function of shear rate in Al₂O₃-water based nanofluids at the volume concentration from 1 to 5% (after 2weeks) [25]

In figure 2.4, viscosity variation with shear rate after 2 weeks of ultrasonication is shown. At any concentration, the behavior is shear thinning at lower shear rates from 0 to 20 s^{-1} i.e., the viscosity value decreases with an increase in shear rate. After a shear rate of 20 s^{-1} , the behavior is almost Newtonian i.e., the viscosity value remains almost constant with an increase in shear rate. Also, the deviation from the Newtonian behavior increases with an increase in volumetric concentration. Therefore, we can conclude that deviation from the Newtonian behavior is more pronounced at lower shear rates and higher volumetric concentrations.

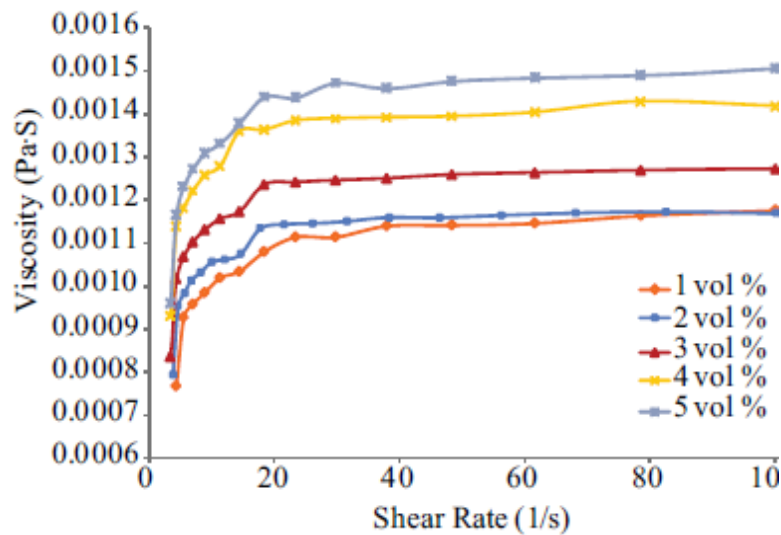


Figure 2.5 Viscosity as a function of shear rate for Al_2O_3 -water based nanofluids at the volume concentrations from 1 to 5% (after re - ultrasonication) [25]

It is seen that after re-ultrasonication (figure 2.5), the behavior is shear thickening at lower shear rates till 20 s^{-1} , i.e., the viscosity increases with the shear rate. At higher shear rates of above 20 s^{-1} value, the behavior again resumed Newtonian. If we compare figure 2.4 and figure 2.5, it can be concluded that the viscosity values are in much lower range after re-ultrasonication. And, also the Non-Newtonian behavior at the lower shear rates is reversed from shear thinning to shear thickening after re-ultrasonication. Therefore, the Sonication plays an important role in determining the Newtonian behavior of Al_2O_3 -water based nanofluids.

2.3 Theoretical Models used to Predict the Dynamic Viscosity of Nanofluid

For the determination of a particle suspension viscosity, there exist few theoretical formulas that can be used. It is very interesting to mention that almost all of the existing

formulas were derived from the Einstein's pioneering work [26] based on the assumption of a linearly viscous fluid that contains dilute suspended spherical particles. He has calculated the energy dissipated by the fluid flow around a single particle and then, by associating that energy with the work done for moving this particle relatively to the surrounding fluid, he obtained:

$$\frac{\mu_{nf}}{\mu_{bf}} = \left(1 + \frac{5}{2}\phi\right) \quad (2.1)$$

where ϕ and μ are, respectively, particle volume fraction and fluid dynamic viscosity; the subscripts bf, nf and r refer respectively to the base-fluid, the nanofluid and to the 'nanofluid-to base fluid' ratio of viscosity. This famous formula was found valid for a very low particle volume fraction, say 0.02 approximately. Since the publication of Einstein's work, there are many interesting and theoretical works all devoted to provide some 'corrections' to his formula. In these works, their authors have considered a negligible inertial effect in the fluid, which has rendered linear the equations of motion.

Brinkman [27] has extended the Einstein's formula to a moderate particle volume concentration, say for concentration lower than 4%. His formula is as follows:

$$\frac{\mu_{nf}}{\mu_{bf}} = \frac{1}{(1-\phi)^{2.5}} \quad (2.2)$$

Frankel and Acrivos [28] have proposed:

$$\frac{\mu_{nf}}{\mu_{bf}} = \frac{9}{8} \left[\frac{(\phi/\phi_m)^{1/3}}{1 - (\phi/\phi_m)^{1/3}} \right] \quad (2.3)$$

where ϕ_m is the maximum particle fraction that must be determined experimentally.

Lundgren [29] has proposed the following equation under the form of the Taylor series in ϕ :

$$\frac{\mu_{nf}}{\mu_{bf}} = (1 + 2.5\phi + 6.25\phi^2 + O(\phi^3)) \quad (2.4)$$

It is obvious that when the terms of second or higher order of ϕ is neglected, this formula simply reduces to Einstein's one.

Batchelor [30] considered the effect due to the Brownian motion of particles for an isotropic suspension of rigid and spherical particles, and proposed:

$$\frac{\mu_{nf}}{\mu_{bf}} = (1 + 2.5\phi + 6.5\phi^2) \quad (2.5)$$

Graham [31] has proposed a generalization form of Eq. (31). His formula, which agrees well with Einstein's one for low value of ϕ , is as follows:

$$\frac{\mu_{nf}}{\mu_{bf}} = \left(1 + 2.5\phi + 4.5 \times \frac{1}{\left(\frac{h}{d_p}\right)\left(2+\frac{h}{d_p}\right)\left(1+\frac{h}{d_p}\right)^2} \right) \quad (2.6)$$

where d_p and h are respectively the particle radius and interparticle spacing.

Eilers [32]

$$\frac{\mu_{nf}}{\mu_{bf}} = \left(1 + \frac{1.25\phi_p}{1-\phi_p/0.78} \right) = 1 + 2.5\phi_p + 4.75\phi_p^2 + \dots \quad (2.7)$$

Eilers model for the prediction of viscosity is based on the experimental data. It is obtained from the curve fitting of experimental data. And, also it is valid for the suspensions of bitumen spheres.

Saito [33]

$$\frac{\mu_{nf}}{\mu_{bf}} = \left(1 + \frac{2.5}{1-\phi_p} \phi_p \right) = 1 + 2.5\phi_p + 2.5\phi_p^2 + \dots \quad (2.8)$$

Saito developed the viscosity model based on the theory for spherical solute-molecules in which a single solute-molecule is placed in the field of flow, obtained by averaging over all the possible positions of a second solute-molecule. It is valid for spherical rigid particles and takes into account the Brownian motion. It shows close prediction only for very small particles.

It is apparent from the above formulas that the effective viscosity of a viscous fluid containing suspended solid particles is function only of the base fluid viscosity and the particle volume fraction. This viscosity enhancement of nanofluids with volume fraction has been cited in literature, but again, there is no agreement about the underlying physical reasons for this behavior. Several authors have proposed semi-empirical equations to describe the enhancement of the viscosity of concentrated suspensions as a function of the volume fraction only, inspired by the original expression of Einstein [26] who derived a linear relation. This classical approach largely underestimates the usual nanofluid viscosities. Nevertheless, many authors followed this approach, proposing similar correlations with variable degree volume fraction polynomials. It can be seen from the theoretical as well as the experimental results (figure 2.6) that the relative viscosity of nanofluids increases with an increase in concentration and, the rate of increase is more pronounced at higher concentrations. It can also be observed, that the classical theoretical

models largely underestimate the nanofluid viscosities i.e., the relative viscosities estimated by the classical models are in the lower range as compared with the experimental results.

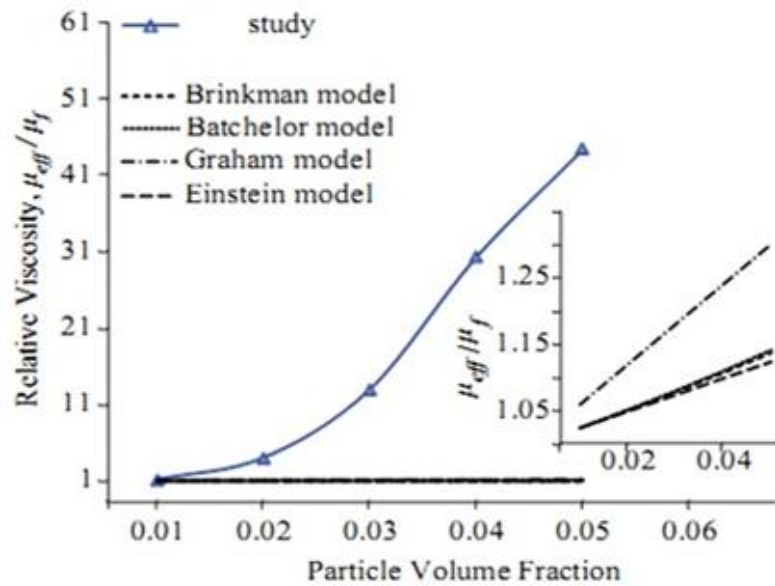


Figure 2.6 Relative viscosity of Al_2O_3 -water based nanofluids as a function of volumetric concentration [25]

Therefore, the classical models cannot be used for the estimation of viscosity values as needed in the design problems. Either, the assumptions used in the formulation of classical models are to be modified or, there is need for the formulation of a new theoretical model which could satisfy the experimental results.

EXPERIMENTAL SETUP

The following are the apparatus or the equipments which are used in the study of the $\text{Al}_2\text{O}_3 - \text{H}_2\text{O}$, (EG + H_2O) based nanofluids.

3.1 Transmission Electron Microscope (TEM)

Electron Microscopes were developed due to the limitations of Light Microscopes which are limited by the physics of light to 500x or 1000x magnification and a resolution of 0.2 micrometers. The Transmission Electron Microscope (TEM) is a type of Electron Microscope and is patterned exactly on the Light Transmission Microscope except that a focused beam of electrons is used instead of light to examine the specimen.

The basic steps involved in all EMs regardless of type are:

- A stream of electrons is formed (by the Electron Source) and accelerated toward the specimen using a positive electrical potential.
- This stream is confined and focused using metal apertures and magnetic lenses (condenser) into a thin, focused, monochromatic beam.
- This beam is focused onto the sample using a magnetic lens.
- Interactions occur inside the irradiated sample, affecting the electron beam.
- These interactions and effects are detected and transformed into an image, which contains information such as structure and composition.

3.2 Scanning Electron Microscope (SEM)

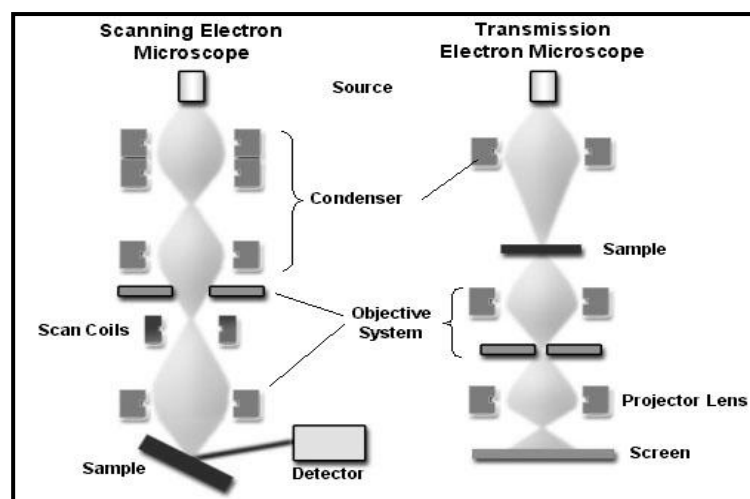


Figure 3.1 Comparisons of SEM and TEM

Scanning Electron Microscopy (SEM) is different from TEM because in SEM, the electron beam is not projected through the whole sample area. Instead, it is raster-scanned across the surface, and the secondary electrons, or x-rays, emitted from the surface are recorded. This generates a lower-resolution image, but allows the direct mapping of surface features, and can even be used for elemental analysis (by study of the x-rays). Figure 3.2 shows the difference between SEM and TEM. From SEM and TEM images, the nanoparticles sizes are determined.

3.3 X- Ray Diffraction (XRD)

XRD is a nondestructive and does not require elaborate sample preparation, so it is widely used in materials characterization. The diffraction patterns are used to find the material, phase of the material and also to determine the interplanar distances in a particular crystal. In the present experimental work, the XRD is used for finding the material and phase identification of the Al_2O_3 nanoparticles used. XRD gives the diffraction pattern of the sample tested. The diffraction pattern is basically X-Y plot with diffracted angle 2θ on its X- axis and intensity of the diffracted beam on its Y- axis. Every material has a unique diffraction pattern with diffraction occurring at unique crystal planes. Therefore, the diffraction pattern of sample being tested is matched with the diffraction pattern of the known materials. The diffraction pattern of the known material to which it matches gives the material and the phase of the material being tested.

The underlying principle of the X- ray diffraction is as follows. In a crystalline solid, the constituent particles (atoms, ions or molecules) are arranged in a regular order. An interaction of a particular crystalline solid with X-rays helps in investigating its actual structure. Crystals are found to act as diffraction gratings for X-rays and this indicates that the constituent particles in the crystals are arranged in planes at close distances in repeating patterns. The X-ray diffraction by the crystal is shown in the figure 3.3.

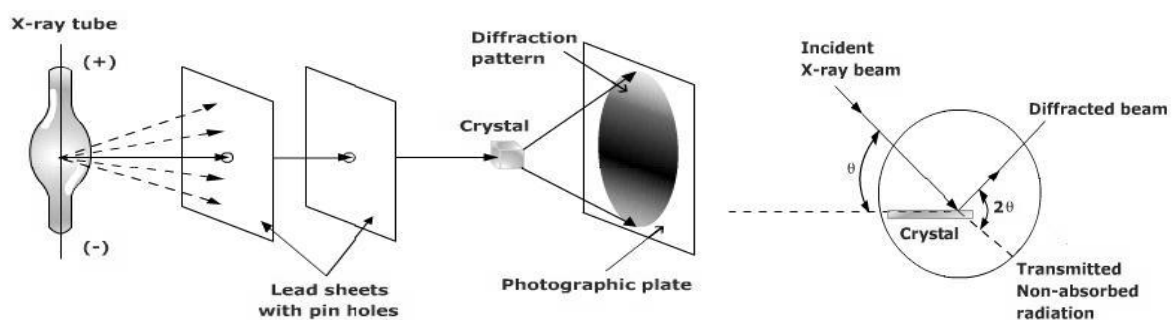


Figure 3.2 X - ray diffraction by crystal

The process is based upon the principle that a crystal may be considered to be made up of a number of parallel equidistant atomic planes, as represented by lines AB, CD and EF in the below figure. In XRD, a collimated beam of X-rays, with a wavelength typically ranging from 0.7 to 2 Å, is incident on a specimen and is diffracted by the crystalline phases in the specimen according to Bragg's law:

$$n \lambda = 2d \sin \theta$$

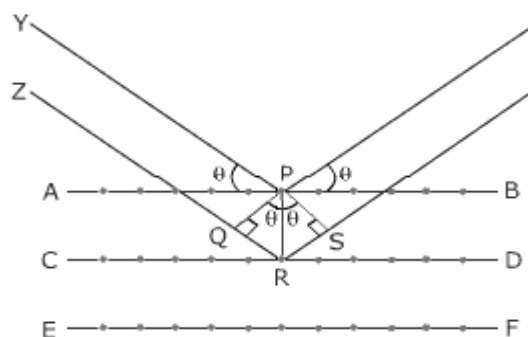


Figure 3.3 X-ray diffraction technique

Where d is the spacing between atomic planes in the crystalline phase and λ is the X-ray wave length. The intensity of the diffracted X-rays is measured as a function of the diffraction angle 2θ and the specimen's orientation. Thus, Bragg's law is a mathematical equation that establishes a relationship between wavelengths of the incident X-ray, the distance between the layers and the angle of diffraction. Bragg's equation can be used to calculate the distances between repeating planes of the particles in a crystal. The XRD of the nanoparticles used is done at the Punjab University, Chandigarh.

3.4 Sonicator



Figure 3.4 Oscar ultrasonicator

The small particle size dramatically increases the surface to volume ratio of the system. In order to increase the surface area of a material energy must be input into the system. This energy is input by dispersing the particles with the help of a device known as Sonicator. The Oscar Ultrasonicator is used for dispersing the Al₂O₃ nanoparticles in the base fluids EG and (EG and water mixture). It is shown in figure 3.6. The model of the Sonicator used is PR - 250MP. It consists of three main components as shown in the figure 3.6. The leftmost component shown is the Controller. In this component, there are start and stop buttons for starting or stopping the sonicator. And, also we can set the maximum temperature at which the sonication must stop, but it must be kept in mind that the maximum temperature set must be above the room temperature. The main parameter i.e. the sonication time can also be set in the controller. The sonication time used in our experiment is 3.5 hours. Apart from that there are two parameters PT ON and PT OFF. The PT ON represents the number of seconds for which the sonicator remains ON. And, PT OFF represents the number of seconds for which it remains OFF. And, in the experiment we have set the parameter PT ON to 10 and PT OFF to 1. Therefore, the sonicator stops for 1 second after every 10 seconds. The middle component is the ultrasonic generator or processor. It transforms the AC line power to a high frequency signal that drives a piezoelectric convertor/transducer. The amplitude of the sonication can be controlled by the knob provided on it. The amplitude increases in the clockwise direction of the knob. The ampere meter is also provided on the processor. The rightmost component shown in the figure 3.6 is the sonication chamber. In this there is a piezoelectric transducer with the sonicator tip or probe at its bottom. The material of the sonicator probe is Titanium. The high frequency signal generated by the generator is converted by the transducer to mechanical vibrations due to the characteristics of the internal piezoelectric crystals. The vibration is amplified and transmitted down the length of the horn/probe where the tip longitudinally expands and contracts. The distance the tip travels is dependent on the amplitude selected by the user through the amplitude control knob. And, the height of this tip can be adjusted in accordance with the amount of the sample to be sonicated. For effective sonication, the tip must be dipped in the uppermost layer of the sample to be sonicated. The entire setup of the sonicator probe and the sample is enclosed in a steel casing with thermocol lining inside. The function of this lining is to dampen the sound waves and reduce the noise. In liquids, the rapid vibration of the tip causes cavitation, the formation and violent collapse of microscopic bubbles. The collapse of thousands of cavitation bubbles, releases tremendous energy in the cavitation field.

Objects and surfaces within the cavitations field are processed. The probe tip diameter dictates the amount of sample that can be effectively processed. Smaller tip diameters deliver high intensity sonication but the energy is focused within small, concentrated area. Larger tip diameters can process larger volumes, but offer lower intensity.

3.5 Viscometer



Figure 3.5 Cone and plate type Brookfield LVDV-III-Pro viscometer

Viscosity of the nanofluids used in the experiment is measured by the Cone and Plate type Brookfield programmable viscometer (model: LVDV-III-Pro) connected to a temperature controlled bath which can vary the fluid temperature between -10°C and 100°C . The schematic of the viscosity measurement set-up is shown in the figure 3.7. The spindle used in the setup is CPE-42. This viscometer has a viscosity measurement range between 0.3 and 6000 cP. Total volume of nanofluid required in the flat cup for measurement is 1 ml. All the measurements are performed under steady state conditions. The speed can be varied from 0.01 to 250 rpm. The shear rate can be varied from 0 to 760 (1/s). The “gap” between the cone and the plate must be verified/ adjusted before measurements are made. This is done by moving the plate (built into the sample cup) up towards the cone until the

pin in the center of the cone touches the surface of the plate, and then by separating (lowering) the plate 0.0005 inch (0.013mm). The Brookfield DV-III Ultra Programmable Rheometer measures fluid parameters of Shear Stress and Viscosity at given Shear Rates. Viscosity is a measure of a fluid's resistance to flow. The principle of operation of the DV-III Ultra is to drive a spindle (which is immersed in the test fluid) through a calibrated spring. The viscous drag of the fluid against the spindle is measured by the spring deflection. Spring deflection is measured with a rotary transducer. The viscosity measurement range of the DV-III Ultra (in centipoise or cP) is determined by the rotational speed of the spindle, the size and shape of the spindle, the container the spindle is rotating in, and the full scale torque of the calibrated spring. The operating principle is to drive a vane spindle through the calibrated spiral spring connected to a motor drive shaft. The vane spindle is immersed in the test material. The resistance of the material to movement is measured by observing increasing torque values as the DV-III Ultra motor rotates. The amount of shaft rotation is measured by the deflection of the calibrated spiral spring inside the instrument. Spring deflection is measured with a rotary transducer.

EXPERIMENTAL WORK, RESULTS & DISCUSSIONS

In this chapter, firstly the methodology used for performing the experiment is discussed. In methodology, the various parameters of the experiment are discussed and also the experimental results showing the viscous behavior of Al_2O_3 - (EG) and (EG + H_2O) based nanofluids have been discussed. The term water used in this chapter refers to the distilled water.

4.1 Methodology

The following methodology has been used for performing the experimental work:

- The Al_2O_3 nanoparticles of average size 40 nm purchased from Reinste Nanoventures Noida have been used in the present experimental work.
- The nanofluids used were prepared by the two step method i.e., by dispersing the nanoparticles in the base fluid used.
- In this experiment, the two types of the base fluids- one is ethylene glycol and other one is a mixture of ethylene glycol and water mixed in the ratio of 60:40 by volume are used. Ethylene glycol is antifreeze i.e. it has a low freezing point. Pure ethylene glycol has a freezing point of about $-12\text{ }^\circ\text{C}$, but when it is mixed with water, the freezing point of the mixture gets depressed to $-45\text{ }^\circ\text{C}$. The reason for the depressed freezing point is that, the ethylene glycol disrupts the hydrogen bonding when dissolved in water and neither can readily form a solid crystal structure when the temperature is lowered. Water has a lower viscosity as compared to the ethylene glycol and when water is mixed with ethylene glycol, the resulting mixture has a viscosity lower than pure ethylene glycol. Therefore, 60:40 ratio mixture of ethylene glycol and water by volume has a lower freezing point and a lower viscosity as compared to the pure ethylene glycol. This is the reason for using one of the base fluids as a mixture of water and ethylene glycol.
- The nanoparticles were dispersed in the base fluids in the varying volumetric concentrations by converting the volume concentrations into the mass of nanoparticles by using the law of mixtures formula.
- The correct mass of the nanoparticles as calculated by law of mixtures formula was dispersed in the base fluid by using the Sonicator for 3.5 hours.

- Then, the different types of nanofluids were prepared with varying volumetric concentrations of 0.005 %, 0.01 %, 0.05 %, 0.1 %.
- Finally, the prepared nanofluids were tested in the Brookfield Viscometer for different volumetric concentrations, shear rates and temperatures.
- The experimental readings were taken in the tabular format. Then, for analysis the tabular data was converted into the graphical format.

Constants	Nanoparticles Type	α - Al ₂ O ₃
	Nanoparticles Shape	Spherical
	Nanoparticles Average Size	40 nm
	Sonication Time	3.5 hours
	Surfactant	-----
Variables	Concentration (%)	0, 0.005, 0.01, 0.05, 0.1
	Base Fluid	[EG], [EG+H ₂ O] (60:40) ----- 10ml
	Temperature (°C)	25, 30, 35, 40, 45, 50
	Shear Rate (1/s)	38, 57, 76, 95, 114, 133, 152, 171, 190
Output	Viscosity	
	Shear Stress	

Table 4.1 Constants and variables in the experiment

In table 4.1, the constants, variables and output parameters of the experimental work have been given. As can be seen in the table, the parameters- nanoparticles type, shape, size, sonication time are constants. The parameters- volumetric concentrations, base fluids used, temperature, and shear rate have been varied. And the output parameters are viscosity and shear stress. The nanoparticles used in the experiment have been purchased from Reinste Nanoventures Noida and their physical properties have also been provided by them. The volume of base fluids is taken as 10 ml. The sonication time has been kept constant at 3.5 hours for all the nanofluids prepared. The four volumetric concentrations - 0.005 %, 0.01 %, 0.05 %, and 0.1 % for both the base fluids have been used. The temperature has been varied from 25 °C to 50 °C in steps of 5 °C. The shear rate has been varied from 38 (1/s) to 190 (1/s) in steps of 19 (1/s).

4.2 Characterization

The characterization involves finding the complete characteristics of the nanoparticles used. It consists of finding the physical properties, such as shape, size, density etc. of the nanoparticles used. Also, the material type and its phase identification by using the x- ray analysis. And, the average particle size is found from TEM images.

Particle Shape	Spherical
Average Particle Size	40 nm
Specific Surface	$> 10 \text{ m}^2/\text{g}$
Purity	$> 99.8 \%$
Density	3965 kg/ m^3
X- Ray analysis	$\alpha - \text{Al}_2\text{O}_3$

Table 4.2 Physical properties of alumina nanoparticles

In Table 4.2, the physical properties of alumina nanoparticles are given. As can be seen from the table, the shape of Al_2O_3 nanoparticles is spherical. The average nanoparticles size is 40 nm. The size of the nanoparticles is also confirmed from the TEM image as given in the figure 4.1. The X- Ray analysis shows that the Al_2O_3 nanoparticles are in α - phase. The value of the density is given as 3965 kg/ m^3 . This density value is required for calculating the mass of nanoparticles required for different volumetric concentrations as shown in equation 4.3.

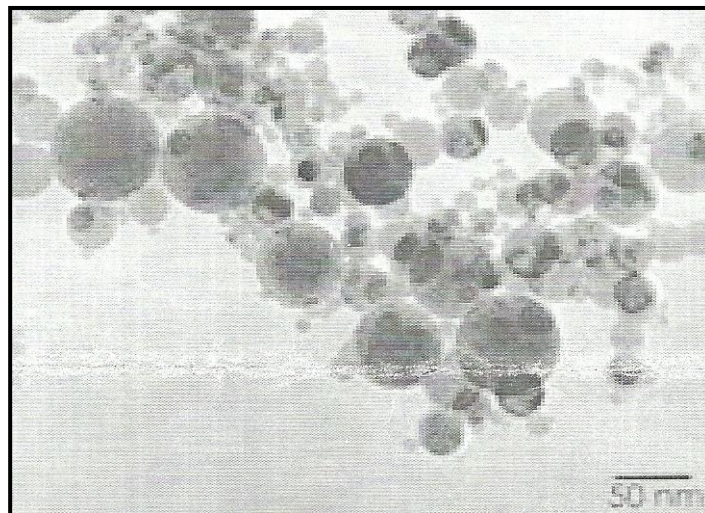


Figure 4.1 TEM image of Al_2O_3 nanoparticles

The figure 4.1 shows the TEM image of Al₂O₃ Nanoparticles. It can be seen from the figure that Al₂O₃ nanoparticles are spherical in shape. Also, majority of the nanoparticles are below 50 nm scale. And, the average nanoparticles size is 40 nm.

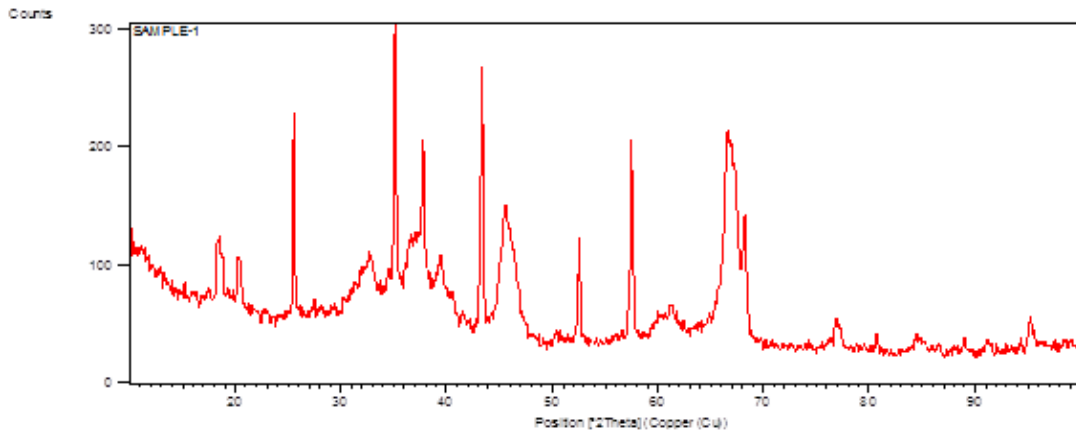


Figure 4.2 XRD pattern image

Pos. [°2Th.]	FWHM [°2Th.]	d-spacing [Å]	Rel. Int. [%]	Area [cts*°2Th.]
18.3415	0.3346	4.83718	23.03	16.97
20.3299	0.3346	4.36834	18.57	13.68
25.5897	0.1506	3.48115	76.56	25.39
35.1567	0.1840	2.55269	100.00	40.54
37.7988	0.1506	2.38011	54.13	17.96
43.3601	0.2342	2.08687	96.90	50.00
45.5745	0.4684	1.99049	38.28	39.50
52.5742	0.1673	1.74078	38.85	14.32
57.5075	0.1673	1.60263	74.61	27.50
66.5432	0.2676	1.40526	71.05	41.90
68.2521	0.2856	1.37304	44.33	37.70

Table 4.3 Peak list of the XRD pattern image

The XRD pattern image of the nanoparticles used in the experiment is shown in figure 4.2. And, table 4.3 gives the corresponding peak list of the XRD pattern. In the present experimental work the sample was tested for the XRD and the diffraction pattern of the sample was matched with the diffraction pattern of the known materials. And, it matches with the diffraction pattern of the Al₂O₃ - α phase. Therefore, it is confirmed that the nanoparticles used in the experimental work are Al₂O₃ nanoparticles in α phase.

The law of mixtures formulae relating the volumetric concentration with the corresponding mass of the Al₂O₃ nanoparticles required for a given volume of base fluid is given below.

$$\text{Volumetric Concentration (\%)} = \frac{[V_{\text{Alumina}}]}{[V_{\text{Alumina}}] + [V_{\text{Base fluid}}]} \times 100 \quad (4.1)$$

$$\text{Volumetric Concentration (\%)} = \frac{\frac{[M_{\text{Alumina}}]}{\rho_{\text{Alumina}}}}{\frac{[M_{\text{Alumina}}]}{\rho_{\text{Alumina}}} + [V_{\text{Base fluid}}]} \times 100 \quad (4.2)$$

In the above formula, ρ_{Alumina} is taken as 3965 kg/ m³ from the table 4.2. The value of $V_{\text{Base fluid}}$ is taken as 10 ml (10×10^{-6} m³). By fixing the ρ_{Alumina} and the $V_{\text{Base fluid}}$ parameters in the above equation, the equation reduces to only two parameters- Volumetric Concentration (%) and M_{Alumina} . The reduced equation involving only these two parameters is given below:

$$\text{Volumetric Concentration (\%)} = \frac{\frac{[M_{\text{Alumina}}]}{3965}}{\frac{[M_{\text{Alumina}}]}{3965} + [10 \times 10^{-6}]} \times 100 \quad (4.3)$$

From the above equation, the mass of nanoparticles required for preparing the different volume concentrations is calculated.

S. No.	Volumetric Concentration (%)	Mass of nanoparticles (mg)
1	0	0
2	0.005	1.982
3	0.01	3.965
4	0.05	19.835
5	0.1	39.689

Table 4.4 Volumetric concentrations of Al₂O₃ nanoparticles with the corresponding mass

Table 4.4 gives the mass of nanoparticles required for preparing the different volumetric concentrations of Al₂O₃ Nanoparticles. Therefore for preparing the Al₂O₃ nanofluids with varying concentrations of nanoparticles, the above amount of nanoparticles were weighed by using a sensitive mass balance. And, dispersed in 10 ml of the base fluids - [EG] and [EG + H₂O] using a sonicator.

4.3 Results of Al₂O₃ - EG Based Nanofluids

In this section, the experimental results of ethylene glycol based nanofluids at different volumetric concentrations of 0%, 0.005%, 0.01%, 0.05%, 0.1% of alumina nano particles are being discussed. The samples were tested for viscosity at different temperatures in the range 25 °C to 50 °C and without any surfactant.

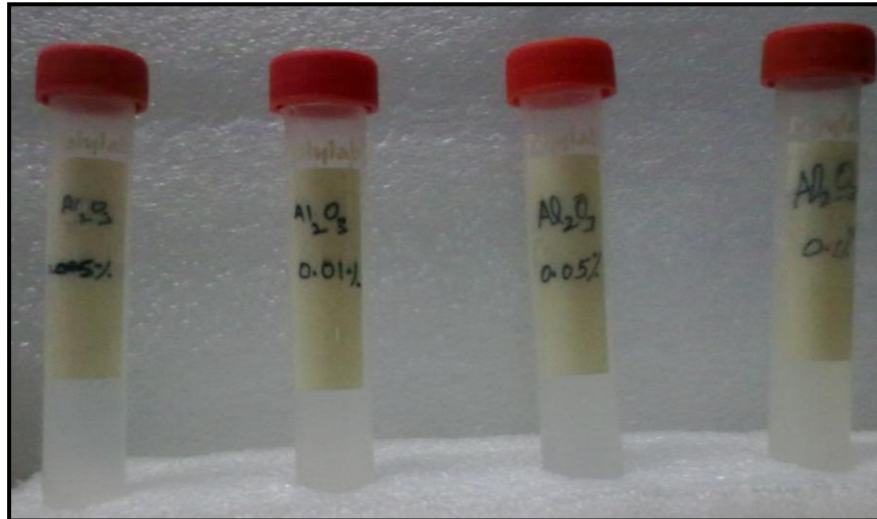


Figure 4.3 Image of the prepared Al₂O₃ - (EG) based nanofluids of different volumetric concentrations

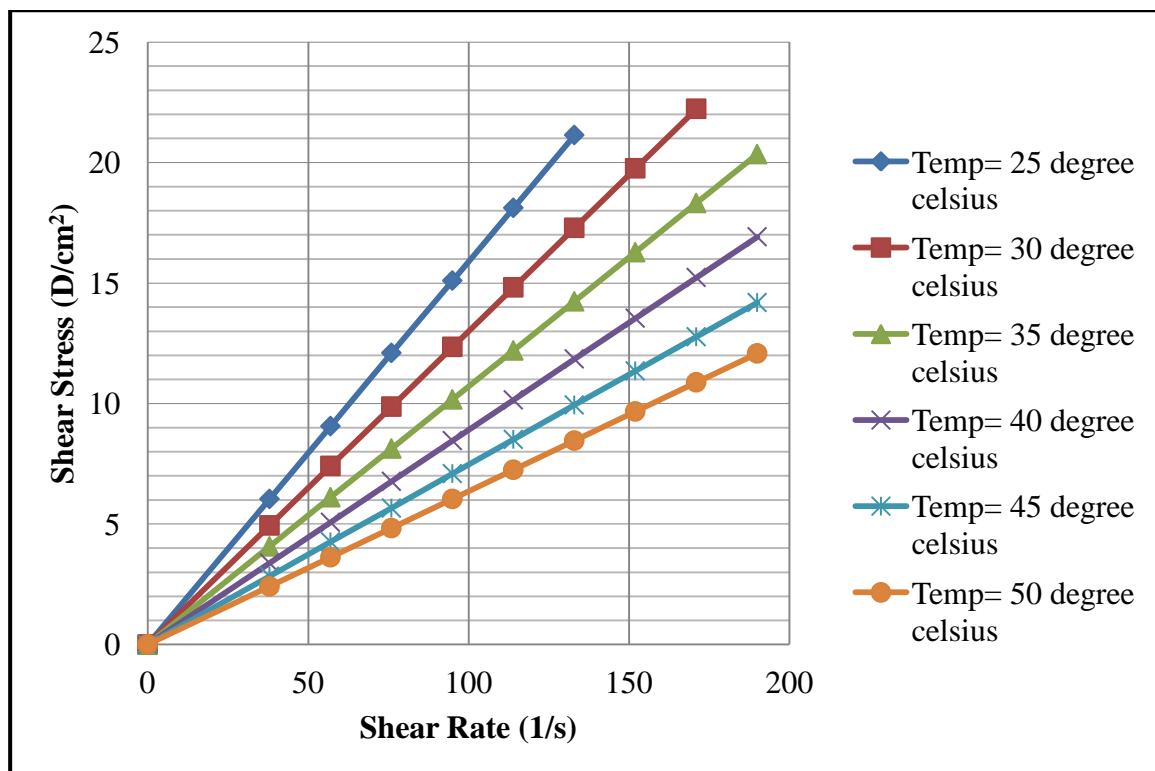


Figure 4.4 Shear stress versus shear rate of pure- EG (0% Al₂O₃ concentration)

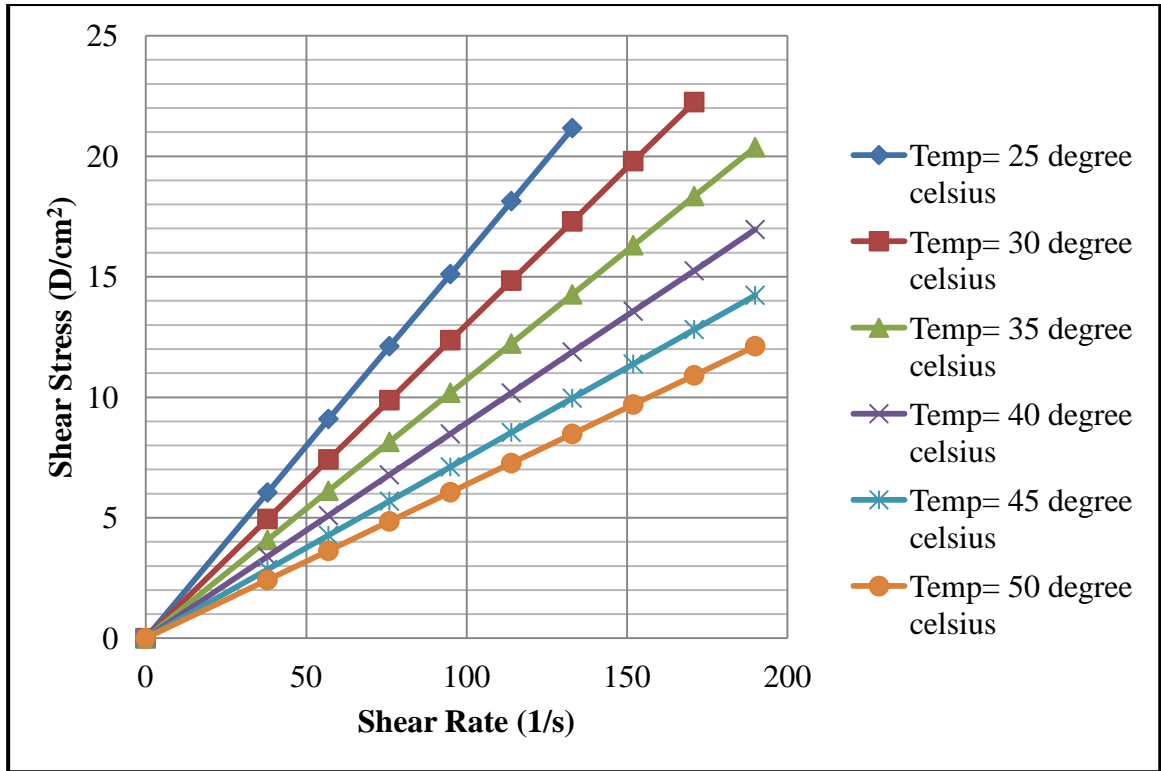


Figure 4.5 Shear stress versus shear rate of Al₂O₃ - EG based nanofluid at a volumetric concentration of 0.005%

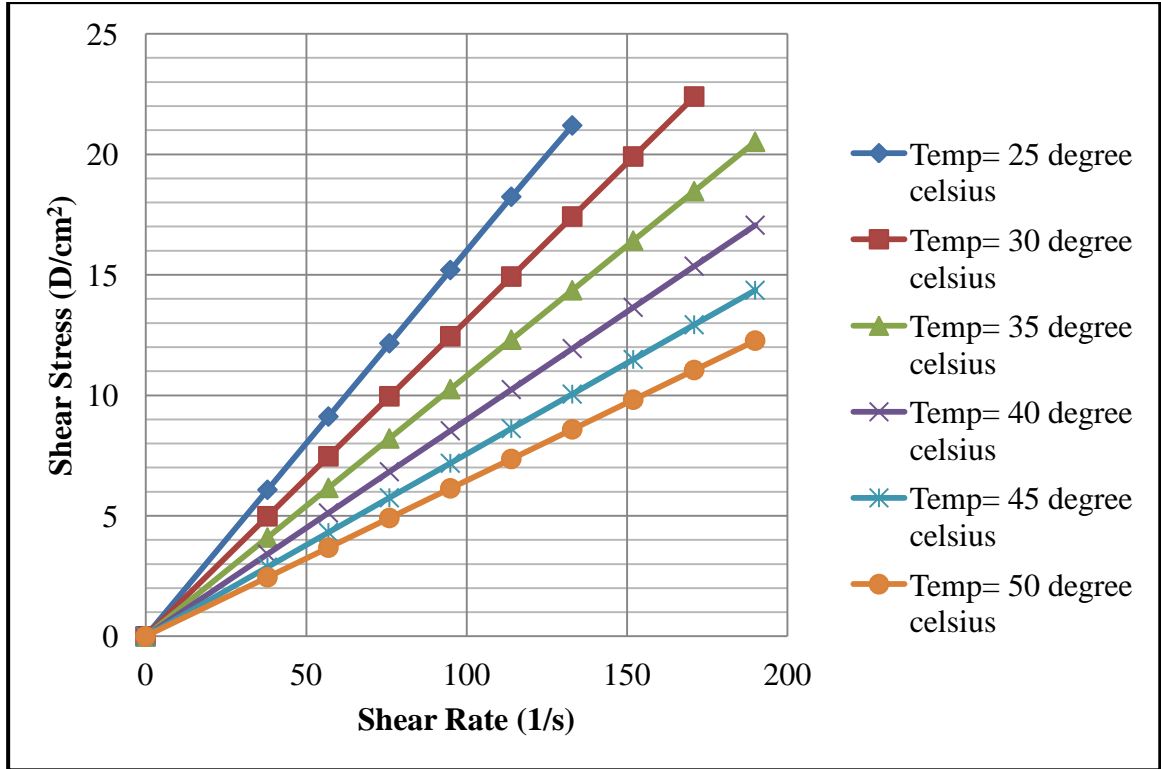


Figure 4.6 Shear stress versus shear rate of Al₂O₃ - EG based nanofluid at a volumetric concentration of 0.01%

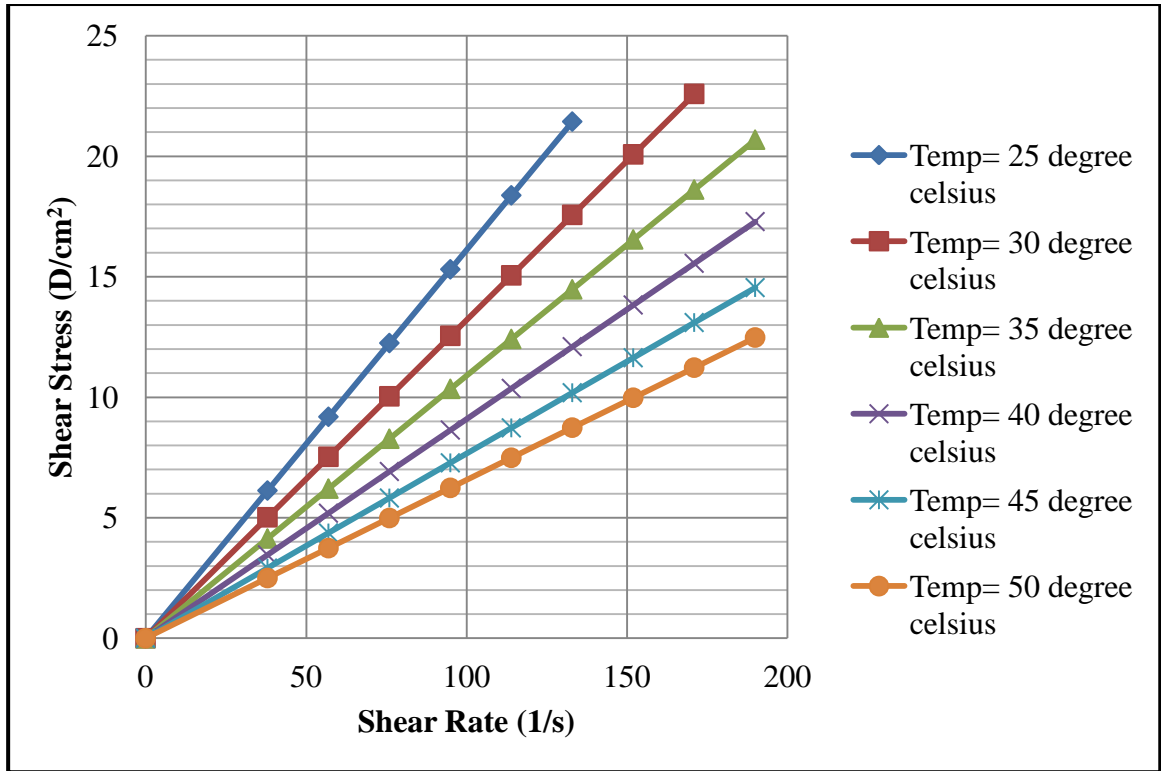


Figure 4.7 Shear stress versus shear rate of Al₂O₃ - EG based nanofluid at a volumetric concentration of 0.05%

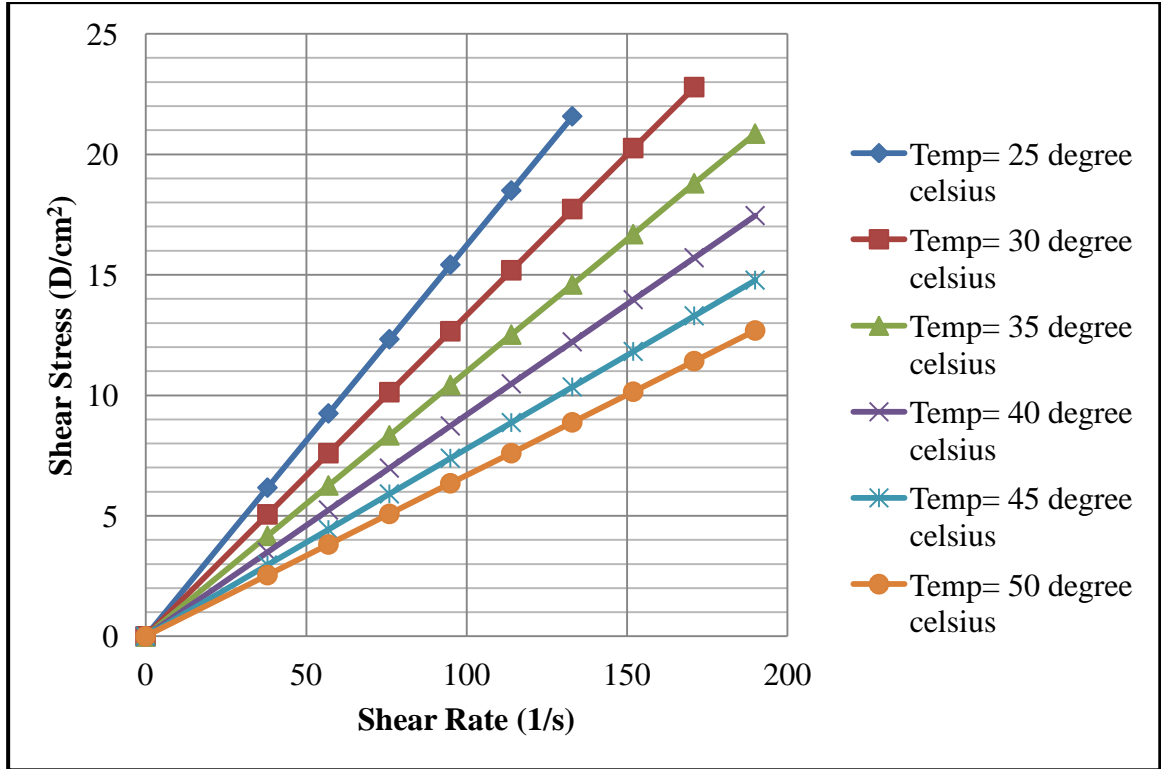


Figure 4.8 Shear stress versus shear rate of Al₂O₃ - EG based nanofluid at a volumetric concentration of 0.1%

Figures 4.4 to 4.8 shows the variation of shear stress with the shear rate at different volumetric concentrations of 0%, 0.005%, 0.01%, 0.05%, 0.1% of Al₂O₃ nanoparticles in ethylene glycol as the base fluid and at different temperatures varied from 25 °C to 50 °C in steps of 5 °C. As it can be seen clearly from figures, that as the shear rate is varied in the range 0 to about 200 (1/s) for all the concentrations, the shear stress changes from 0 to about 25 Dynes/ cm². It is observed that as the shear rate increase the shear stress developed in the fluid also increases. That is, the shear stress is proportional to shear rate for the EG based nanofluids at different volumetric concentrations. And, as the lines of variations are straight lines passing through the origin, therefore the shear stress is directly proportional to the shear rate. Therefore, the Al₂O₃ - EG based nanofluids at all the volumetric concentrations considered above behaves as Newtonian fluid. It can also be seen from the figure that at any concentration the variation trend of shear stress with the shear rate is same for all the temperatures considered. But, the inclination of lines is different at the different temperatures; therefore the rate of variation is different at different temperatures. And the slope of lines decreases with an increase of temperature from the 25 °C to 50 °C. In the case of Newtonian fluids the slope represents the viscosity of the fluids. Therefore, we can conclude that the viscosity is decreasing with an increase in temperature. The base fluid represents the case of 0% concentration and it is also behaving in the same manner as discussed above. Therefore, we can conclude that the addition of Al₂O₃ nanoparticles in the concentrations of 0.005%, 0.01%, 0.05%, 0.1% in the EG as base fluid do not change its Newtonian behavior much.

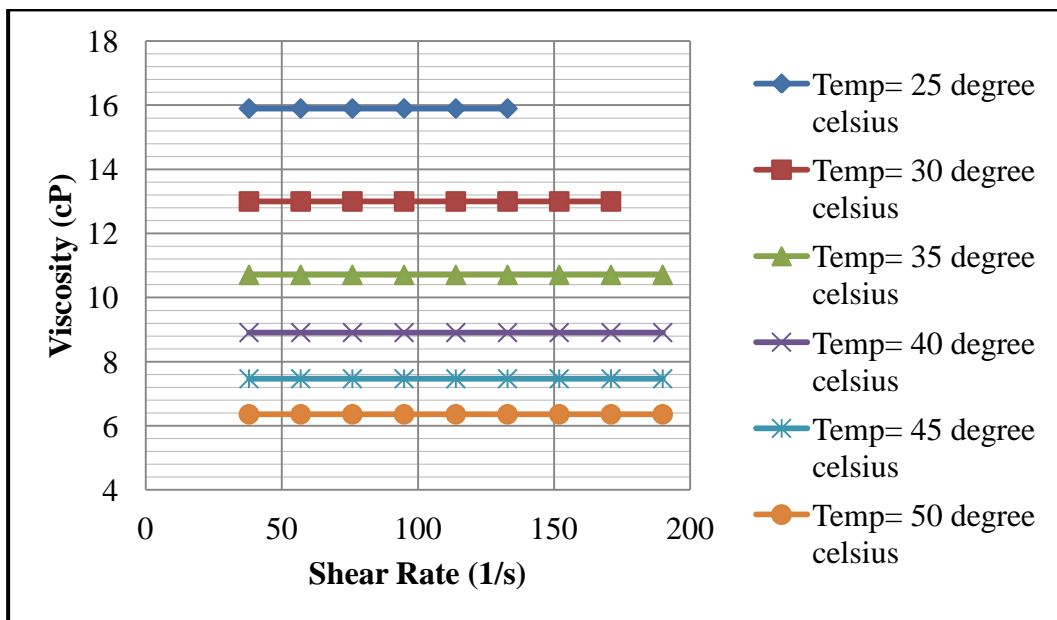


Figure 4.9 Viscosity versus shear rate of pure- EG (0% Al₂O₃ concentration)

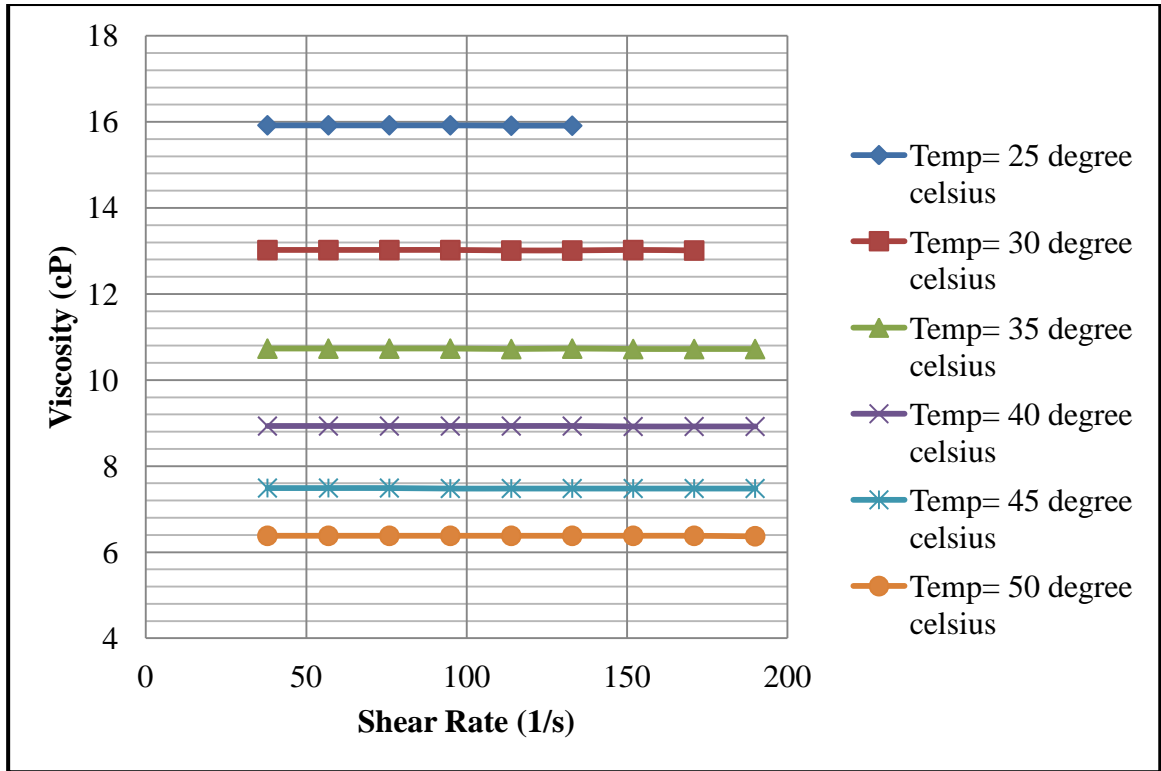


Figure 4.10 Viscosity versus shear rate of Al₂O₃ - EG based nanofluid at a volumetric concentration of 0.005%

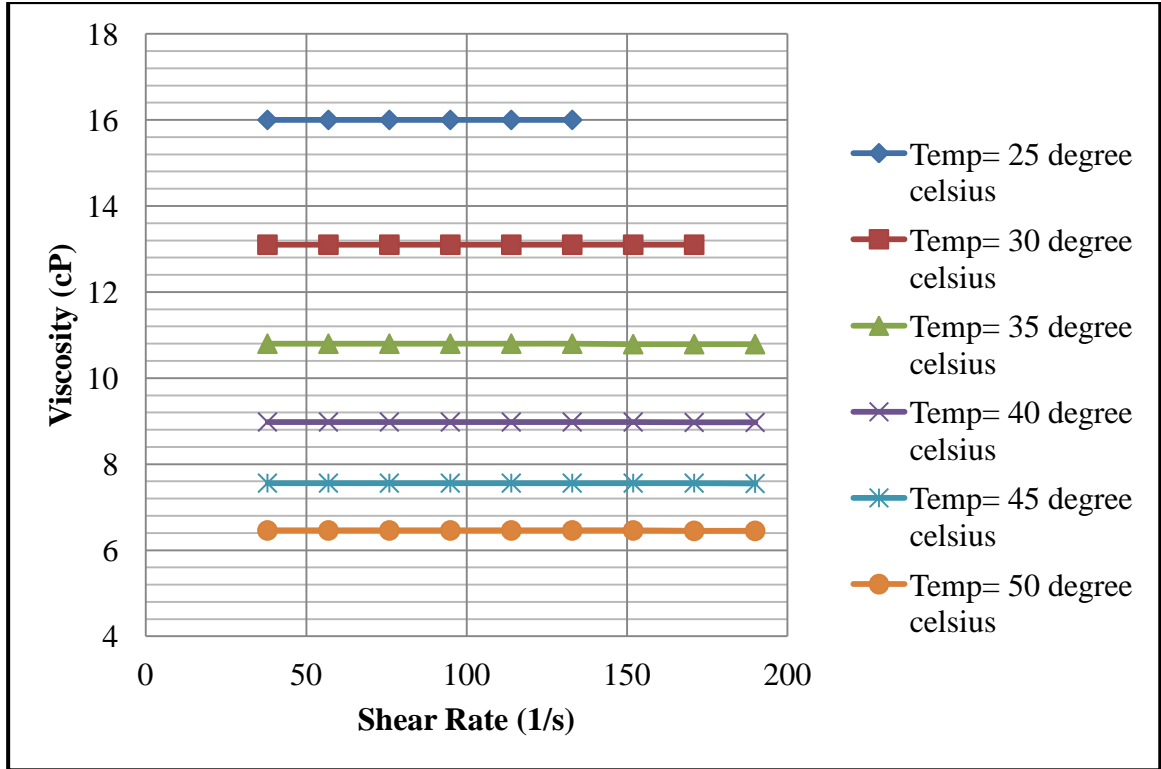


Figure 4.11 Viscosity versus shear rate of Al₂O₃ - EG based nanofluid at a volumetric concentration of 0.01%

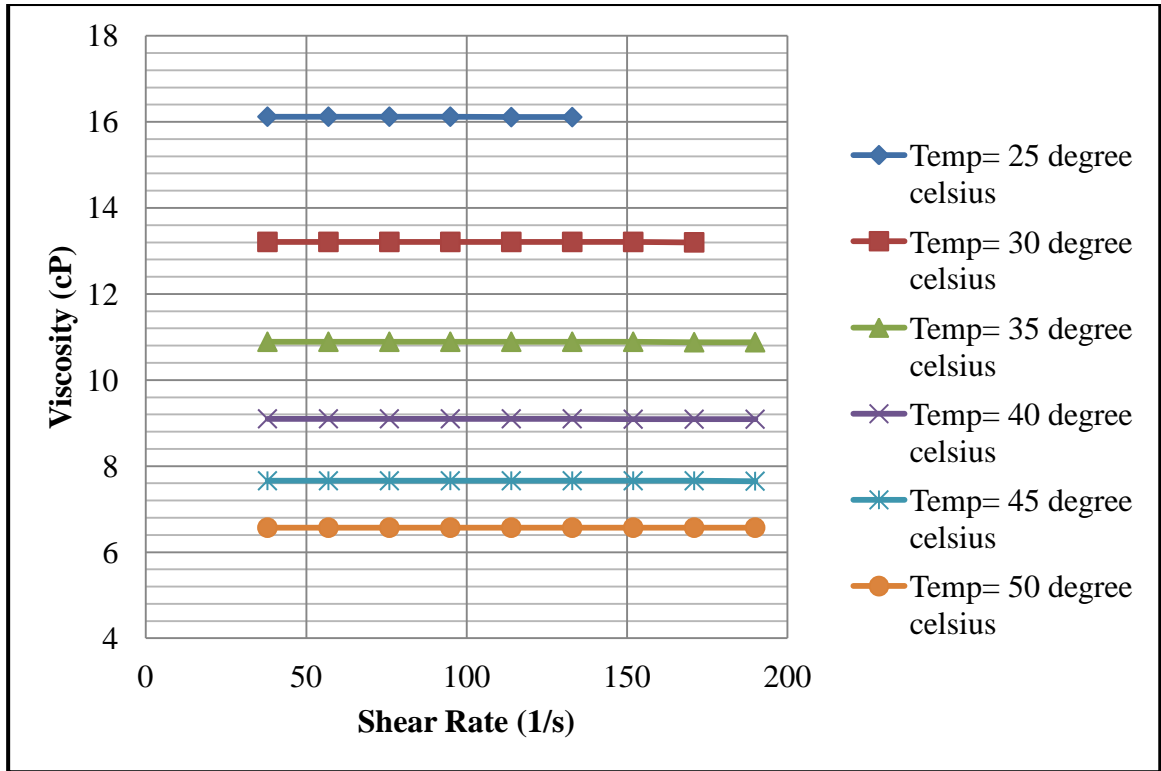


Figure 4.12 Viscosity versus shear rate of Al₂O₃ - EG based nanofluid at a volumetric concentration of 0.05%

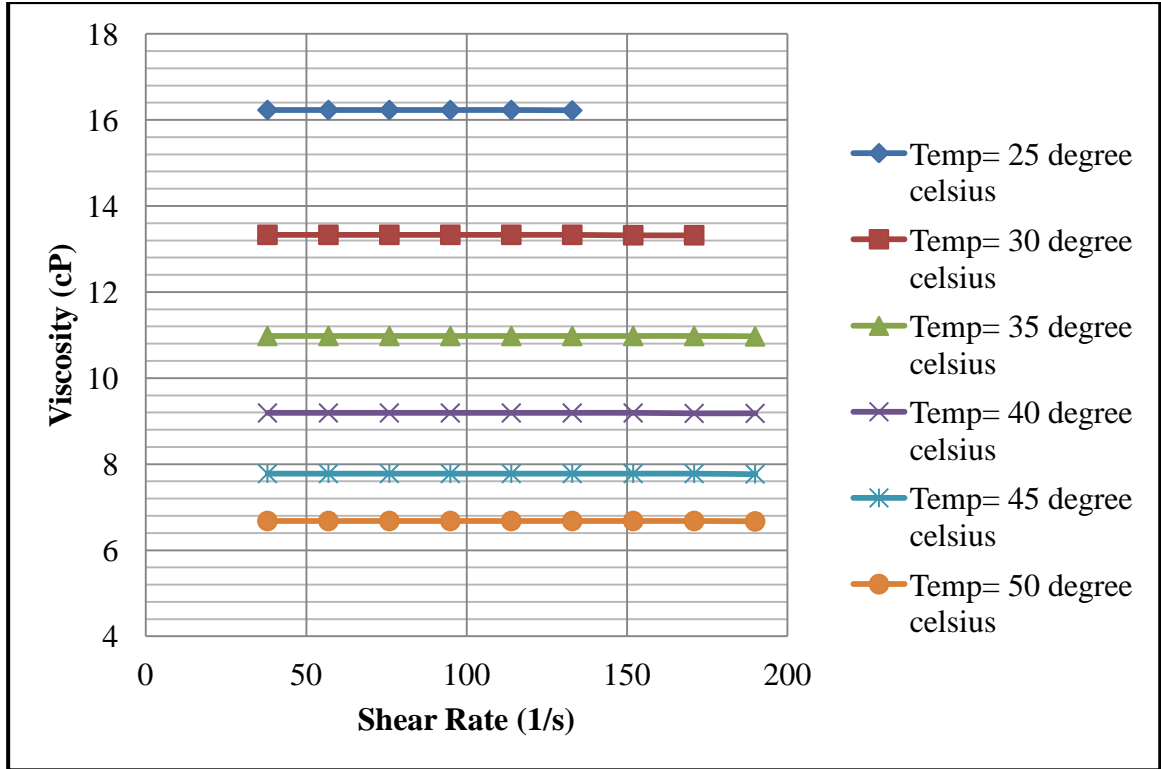


Figure 4.13 Viscosity versus shear rate of Al₂O₃ - EG based nanofluid at a volumetric concentration of 0.1%

Figures 4.9 to 4.13 shows the variation of Viscosity with the Shear Rate at different volumetric concentrations of 0%, 0.005%, 0.01%, 0.05%, 0.1% of Al₂O₃ nanoparticles in ethylene glycol as the base fluid and at different temperatures varied from 25 °C to 50 °C in steps of 5 °C. It can be observed, that as the shear rate is varied in the range 0 to about 200 (1/s) for all the concentrations, the viscosity varies between 16 cP to about 6.5 cP for various concentrations and temperatures. It can also be seen, that at any temperature the viscosity lines are horizontal parallel to the horizontal axis. This implies that at a constant temperature, as the shear rate is increased the viscosity of the fluid remains constant. That is, the viscosity is independent of the shear rate applied. This is the condition for the fluid to be Newtonian. Therefore, the nanofluids considered, behaved as Newtonian. It can also be seen from the figures that at any concentration, the viscosity lines are horizontal at all the temperatures. But these horizontal viscosity lines are at different heights/ levels at different temperatures. This implies that the viscosity is varying with the temperature. And, at any concentration as the temperature increases the height of the lines decreases. The height represents the viscosity of the nanofluid; therefore with an increase in the temperature the viscosity decreases. The base fluid represents the case of 0% concentration and it is also behaving in the same manner as discussed above. Therefore, we can conclude that the addition of Al₂O₃ nanoparticles in the concentrations of 0.005%, 0.01%, 0.05%, 0.1% in the EG as base fluid do not change its Newtonian behavior.

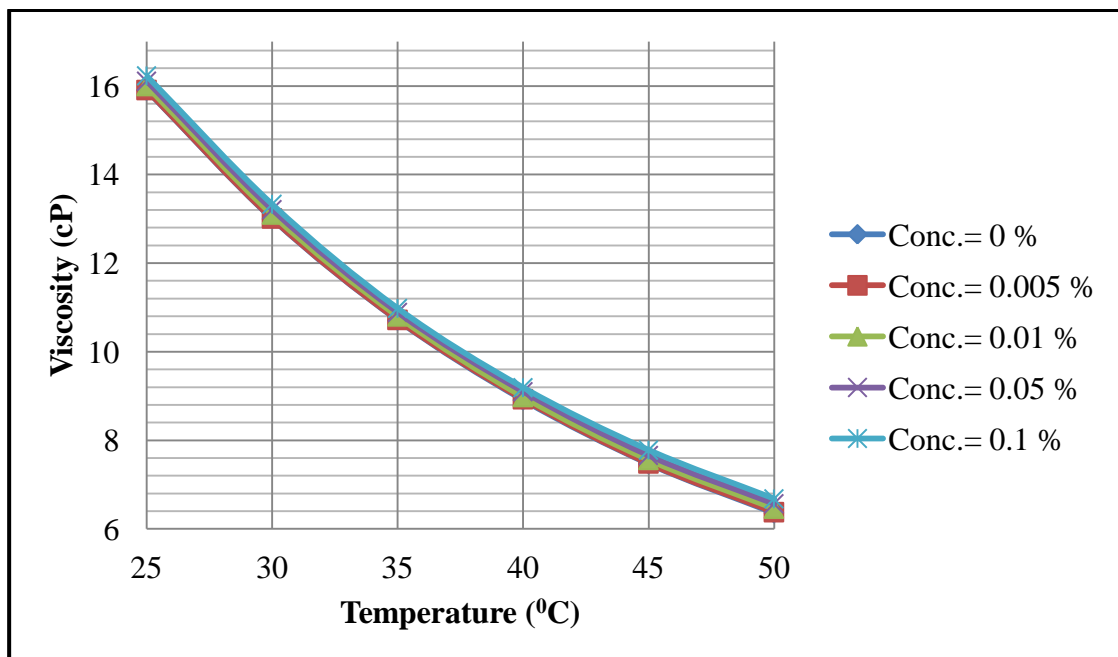


Figure 4.14 Viscosity versus temperature of Al₂O₃ - EG based nanofluids at different volumetric concentrations (at a constant shear rate of 114 /s)

Figure 4.14 shows the variation of viscosity of nanofluids with the temperature at different volumetric concentrations of 0%, 0.005%, 0.01%, 0.05%, 0.1% of Al_2O_3 nanoparticles in Ethylene Glycol as the base fluid and a constant shear rate of 114 (1/s). It can be seen from the figure that as the temperature is varied from 25 $^{\circ}\text{C}$ to 50 $^{\circ}\text{C}$ in steps of 5 $^{\circ}\text{C}$ the viscosity value decreases from about 16 cP to about 6.5 cP. That is, with an increase in temperature the viscosity decreases for each nanofluid concentration considered. This result was also clear from the figures 4.4 to 4.13. But actual variation i.e., whether the viscosity is decreasing linearly or non- linearly with an increase in temperature was not clear. Therefore to study the actual variation of viscosity with temperature, the graph between viscosity and temperature is plotted. Now, it is clear from the figure that the viscosity is decreasing non- linearly with an increase in temperature. It is also seen that the slope of the line at any concentration, decreases as the temperature is increased. The slope represents the rate of variation, therefore we can conclude that the rate of decrease of viscosity is more at the lower temperatures and gradually reduces as the temperature is increased. From the above figure the viscosity variation at different concentrations is not clear, the curves seems to be overlapping. This is because in this experimental work nanofluid with very lower volumetric concentrations are used, which affects the viscosity marginally. But if the experimental data in the tabular format given at the end in the annexure is studied, it can be inferred that the higher concentration curves are above than the lower concentration curves.

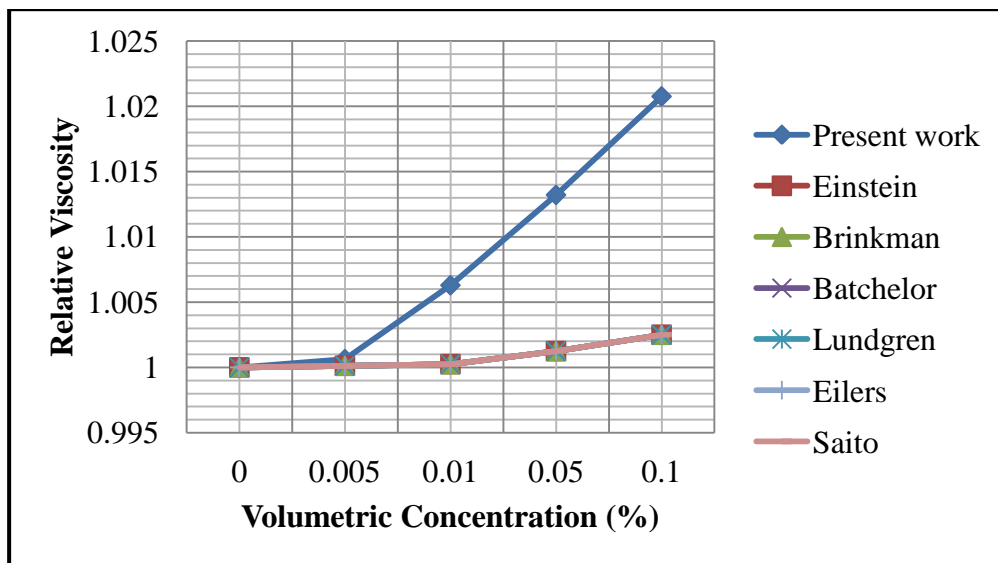


Figure 4.15 Relative viscosity versus volumetric concentration of Al_2O_3 - EG based nanofluids (at a constant shear rate of 114 /s and a constant temperature of 25 $^{\circ}\text{C}$) and its comparison with the theoretical models

As discussed before, the variation of viscosity with concentration was not clear from the figure 4.14. Therefore, to see the variation of viscosity with concentration and to compare with classical theoretical models, a new graph as shown in the figure 4.15 is drawn. Figure 4.15 represents the graph showing the variation of relative viscosity with volumetric concentration for the experimental work (at a constant shear rate of 114 /s and constant temperature of 25 °C) and its comparison with different theoretical models. It must be noted here that the viscosity plotted here is the relative viscosity and is different from the absolute viscosity which was plotted in the earlier plots. The absolute viscosity and relative viscosity are related to each other. And, relative viscosity is defined as the ratio of absolute viscosity and the viscosity of the base fluid. It can be easily seen from the figure that as the volumetric concentration increases the relative viscosity increases. The rate of increase of viscosity with concentration is almost linear. And, it is also seen that the addition of 0.005 % of Al_2O_3 nanoparticles in EG slightly increases the nanofluid viscosity as compared with the other concentrations. It is seen that the theoretical models largely underestimates the viscosity of the nanofluids. And, the underestimation of the viscosity increases with an increase in the concentration. From 0% to 0.005% concentration, the values of viscosity predicted by the models are in close agreement. Therefore, we can conclude that the theoretical models cannot be used for viscosity prediction at higher concentrations.

4.4 Al_2O_3 - (EG + H_2O) Based Nanofluids

In this section the experimental results of ethylene glycol and water mixed in the ratio of 60:40 by volume as the base fluid at different volumetric concentrations of 0%, 0.005%, 0.01%, 0.05%, 0.1% of Al_2O_3 nanoparticles are being discussed.

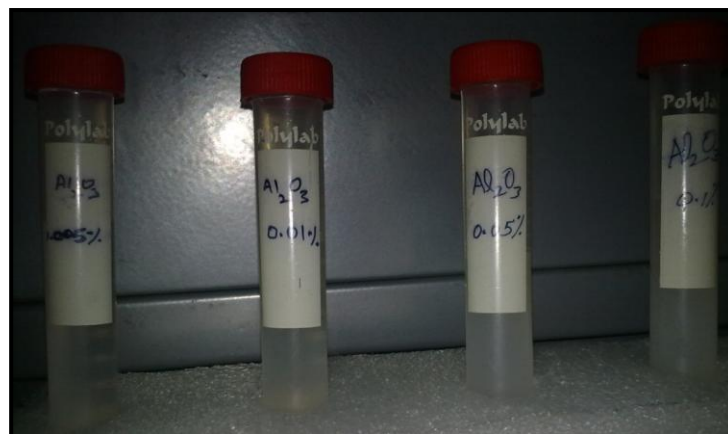


Figure 4.16 Image of the prepared Al_2O_3 - (EG + H_2O) based nanofluids of different volumetric concentrations

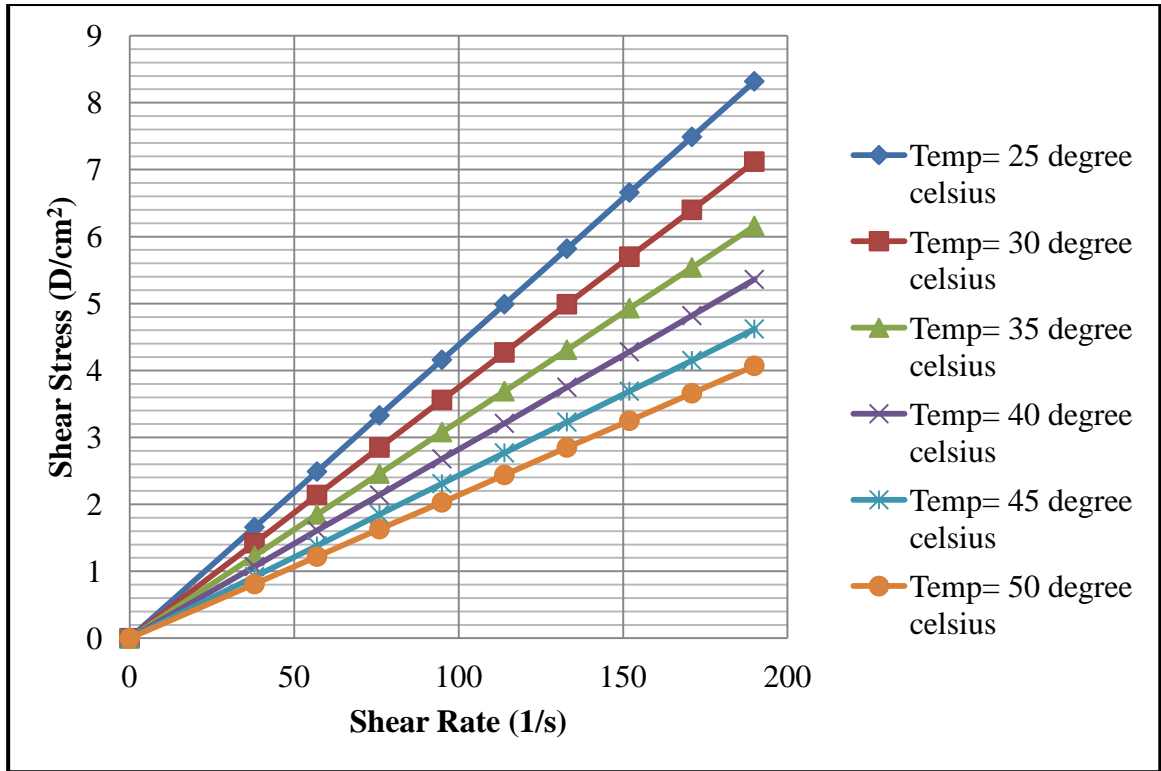


Figure 4.17 Shear stress versus shear rate of pure- (EG + H₂O) (0% Al₂O₃ concentration)

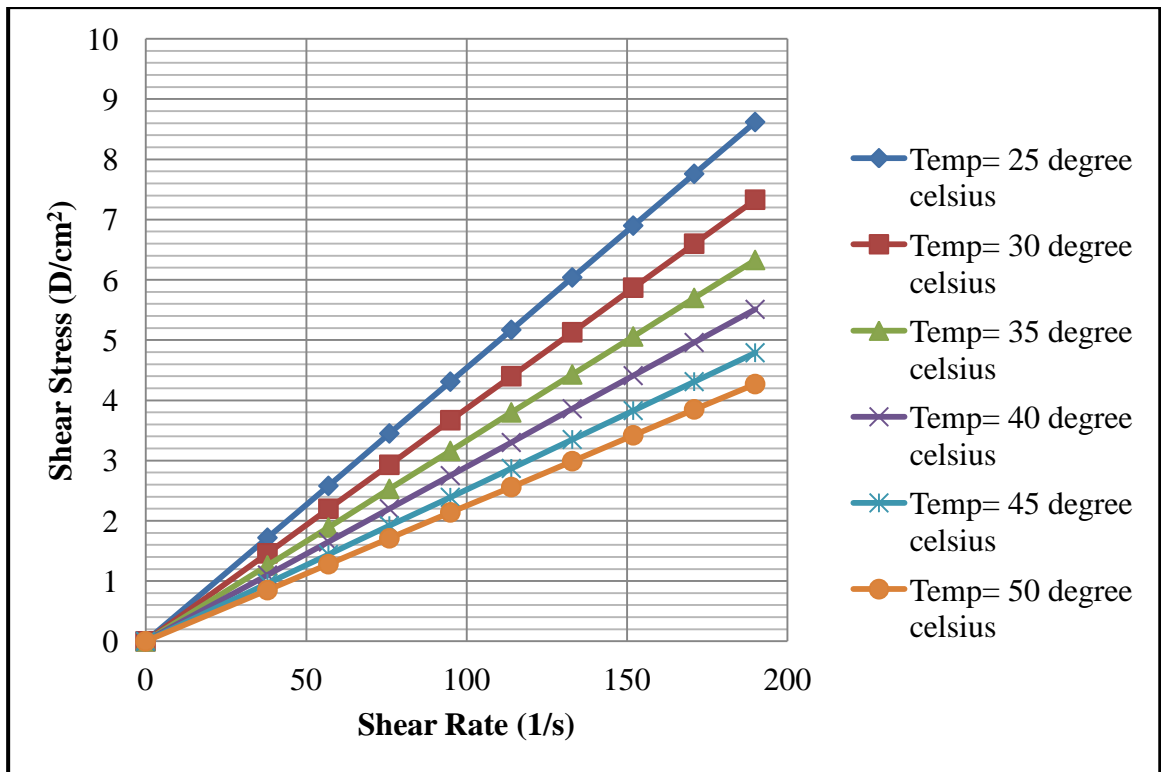


Figure 4.18 Shear stress versus shear rate of Al₂O₃ - (EG + H₂O) based nanofluid at a volumetric concentration of 0.005%

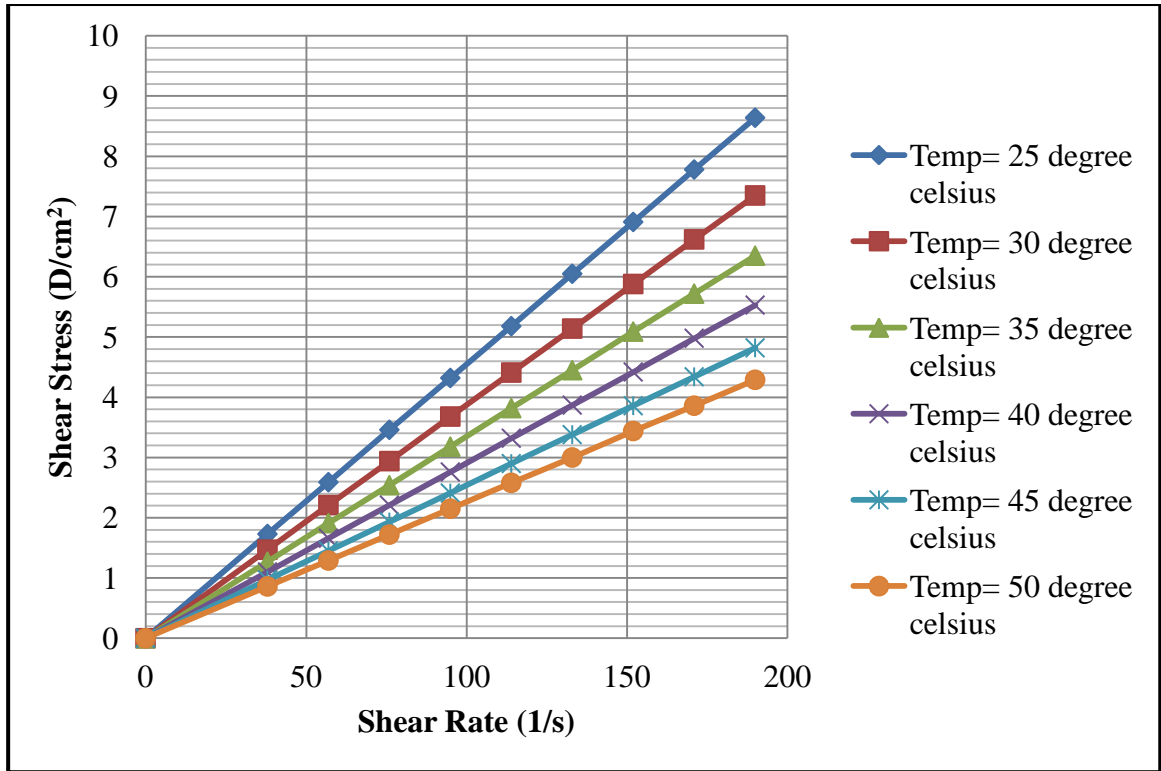


Figure 4.19 Shear stress versus shear rate of Al_2O_3 - (EG + H_2O) based nanofluid at a volumetric concentration of 0.01%

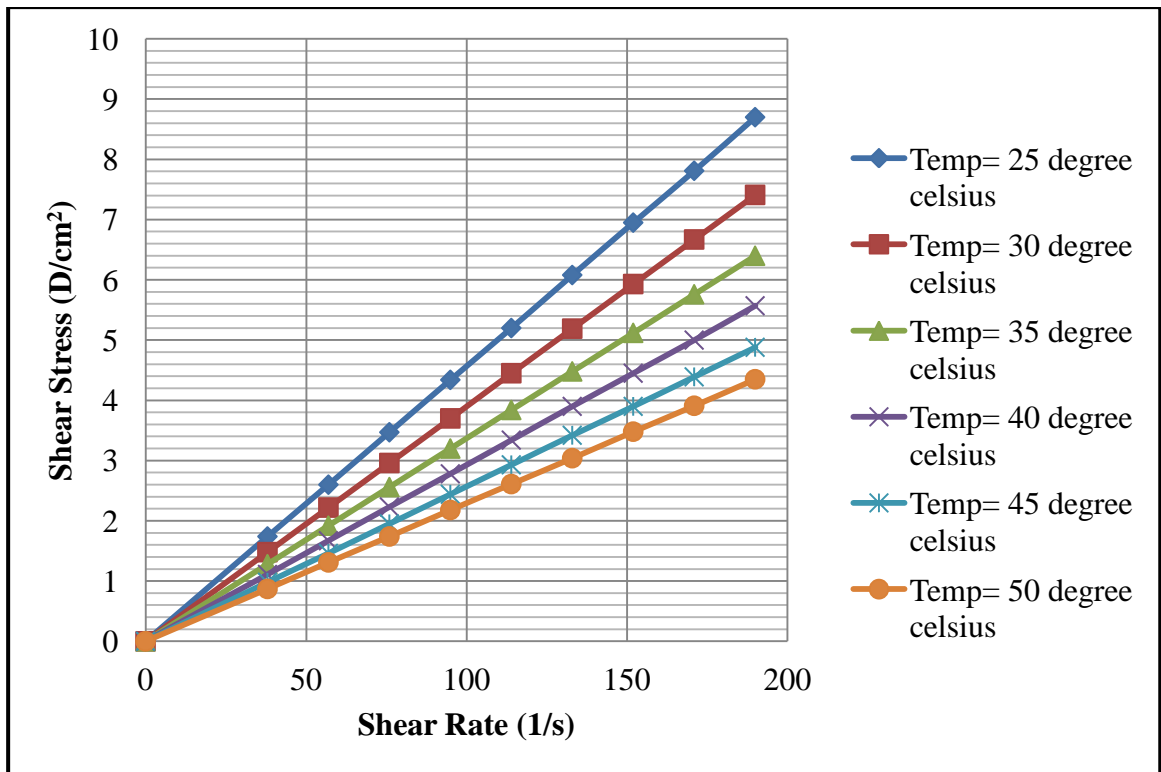


Figure 4.20 Shear stress versus shear rate of Al_2O_3 - (EG + H_2O) based nanofluid at a volumetric concentration of 0.05%

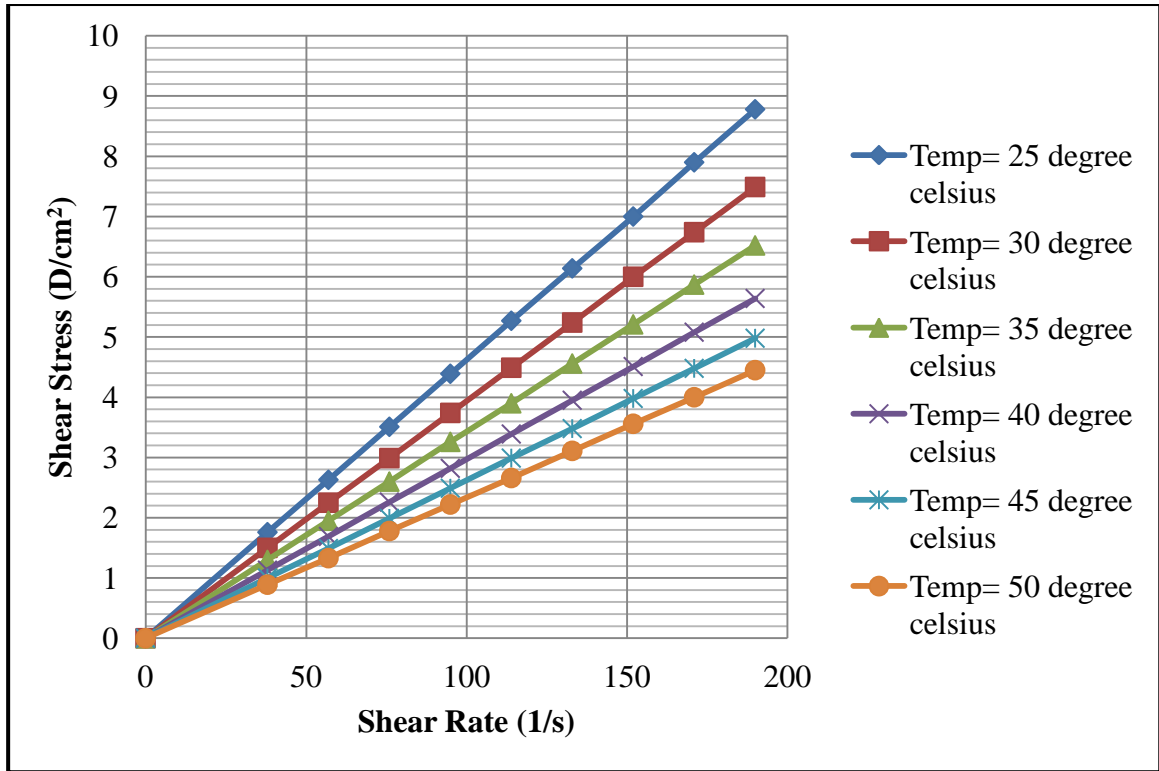


Figure 4.21 Shear stress versus shear rate of Al_2O_3 - (EG + H_2O) based nanofluid at a volumetric concentration of 0.1%

Figures 4.17 to 4.21 shows the variation of Shear Stress with the Shear Rate at different volumetric concentrations of 0%, 0.005%, 0.01%, 0.05%, 0.1% of Al_2O_3 nanoparticles in Ethylene Glycol and water mixture as the base fluid and at different temperatures varied from 25 °C to 50 °C in steps of 5 °C. As can be clearly seen from the figure, that as the shear rate is varied in the range 0 to about 200 (1/s) for all the concentrations, the shear stress changes from about 0 to about 9 Dynes/ cm^2 . It can be seen that as the shear rate is increased the shear stress developed in the fluid also increases. That is, shear stress is proportional to shear rate for the (EG + H_2O) based nanofluids at different concentrations. And, as the lines of variations are straight lines passing through the origin, therefore the shear stress is directly proportional to the shear rate. Therefore, the Al_2O_3 - (EG + H_2O) based nanofluids at all the volumetric concentrations considered above behaved as Newtonian fluid. It is observed that at any concentration the variation trend of shear stress with the shear rate is same for all the temperatures considered. But, the inclination of lines is different at the different temperatures; therefore the rate of variation is different at different temperatures. And the slope of lines decreases with an increase of temperature from the 25 °C to 50 °C. In the case of Newtonian fluids the slope represents the viscosity of nanofluids. Therefore, we can conclude that the viscosity is decreasing with an increase

in temperature. The base fluid represents the case of 0% concentration and it is also behaving in the same manner as discussed above. Therefore, we can conclude that the addition of Al_2O_3 nanoparticles in the concentrations of 0.005%, 0.01%, 0.05%, 0.1% in the (EG + H_2O) as base fluid did not changed its Newtonian behavior.

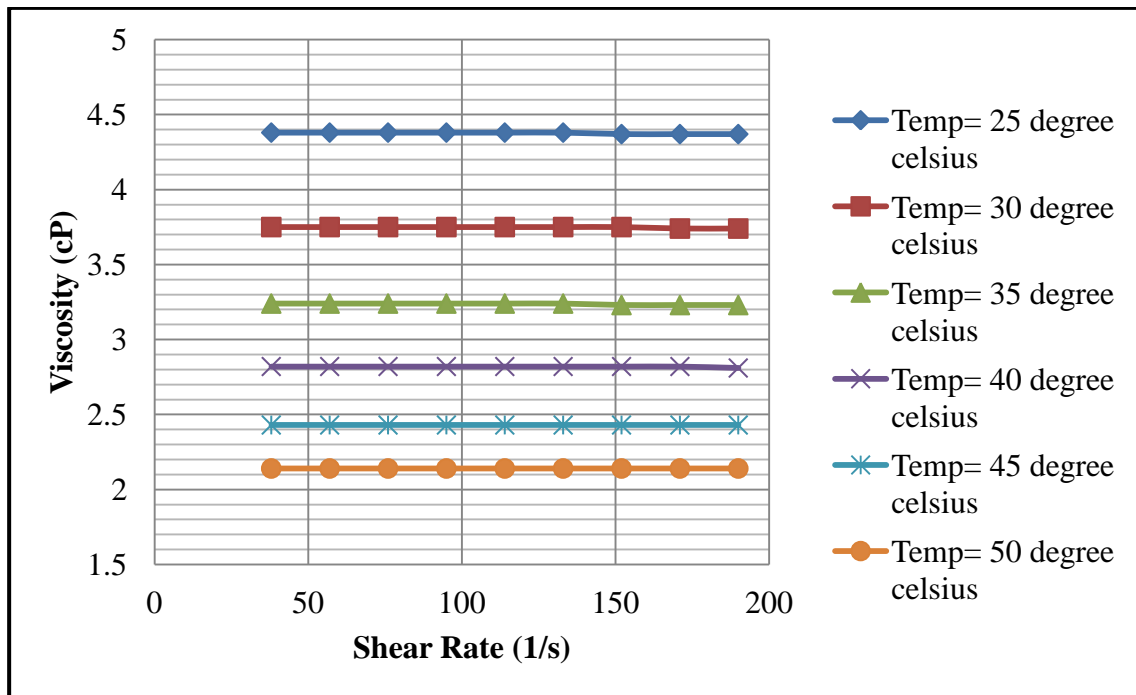


Figure 4.22 Viscosity versus shear rate of pure - (EG + H_2O)

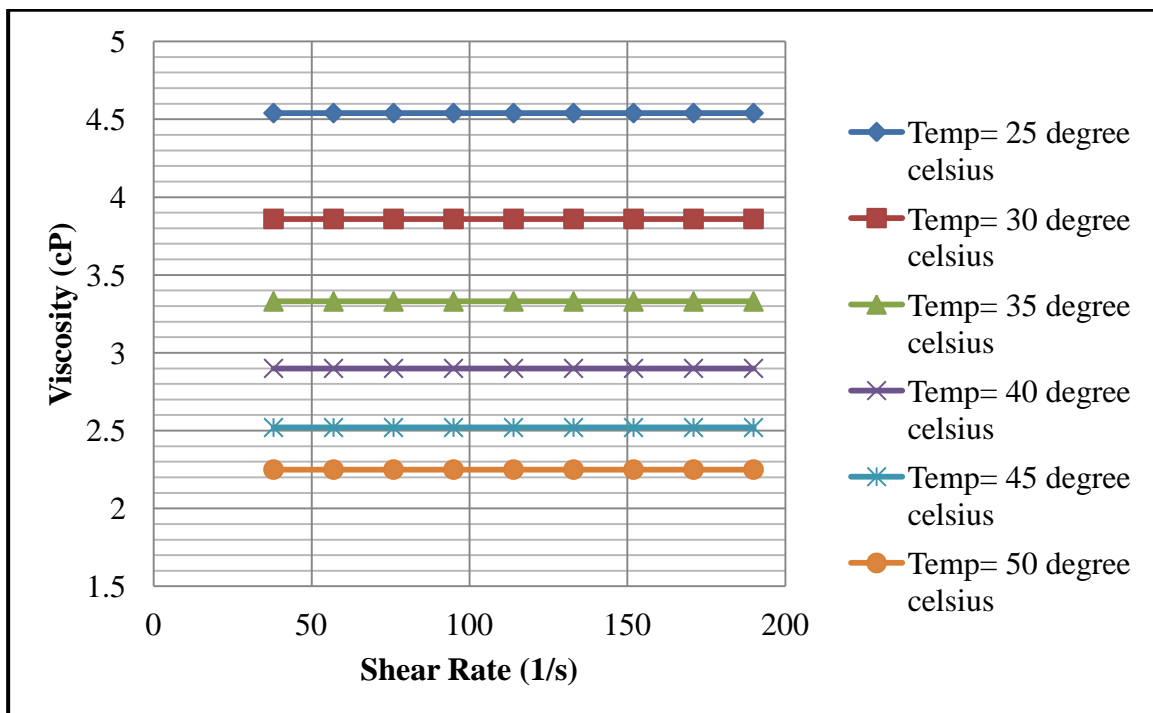


Figure 4.23 Viscosity versus shear rate of Al_2O_3 - (EG + H_2O) based nanofluid at a volumetric concentration of 0.005%

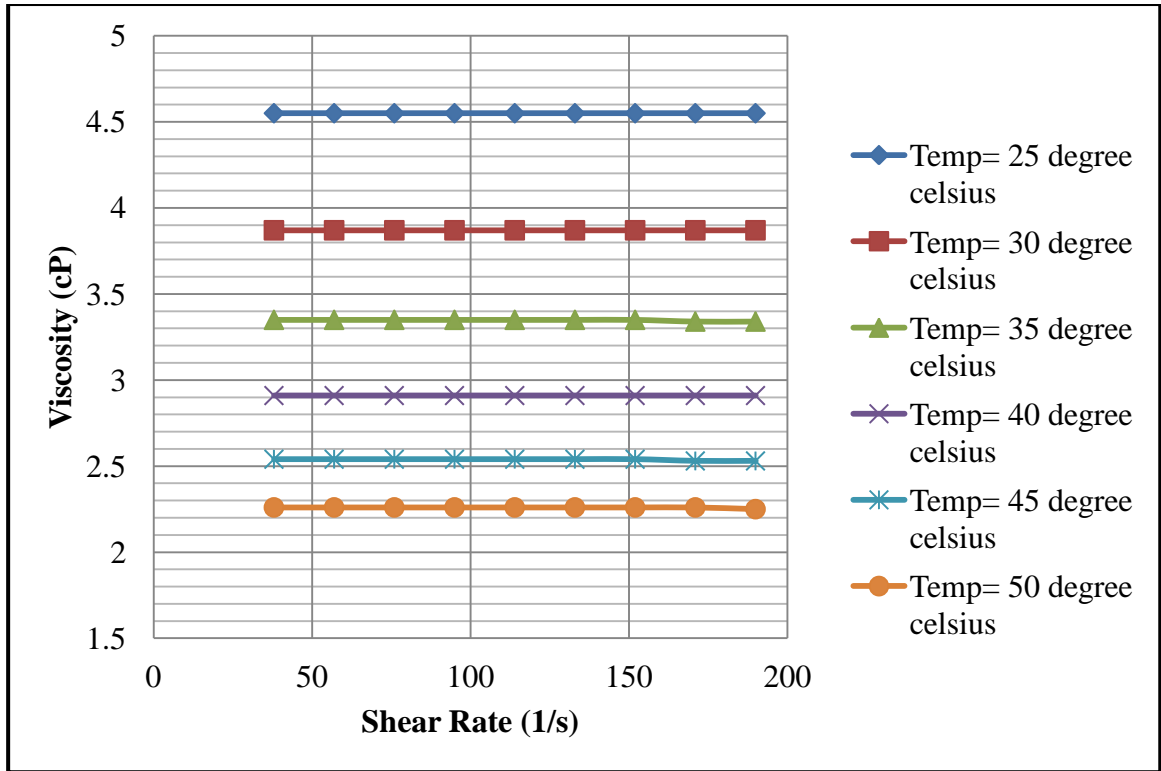


Figure 4.24 Viscosity versus shear rate of Al₂O₃ - (EG + H₂O) based nanofluid at a volumetric concentration of 0.01%

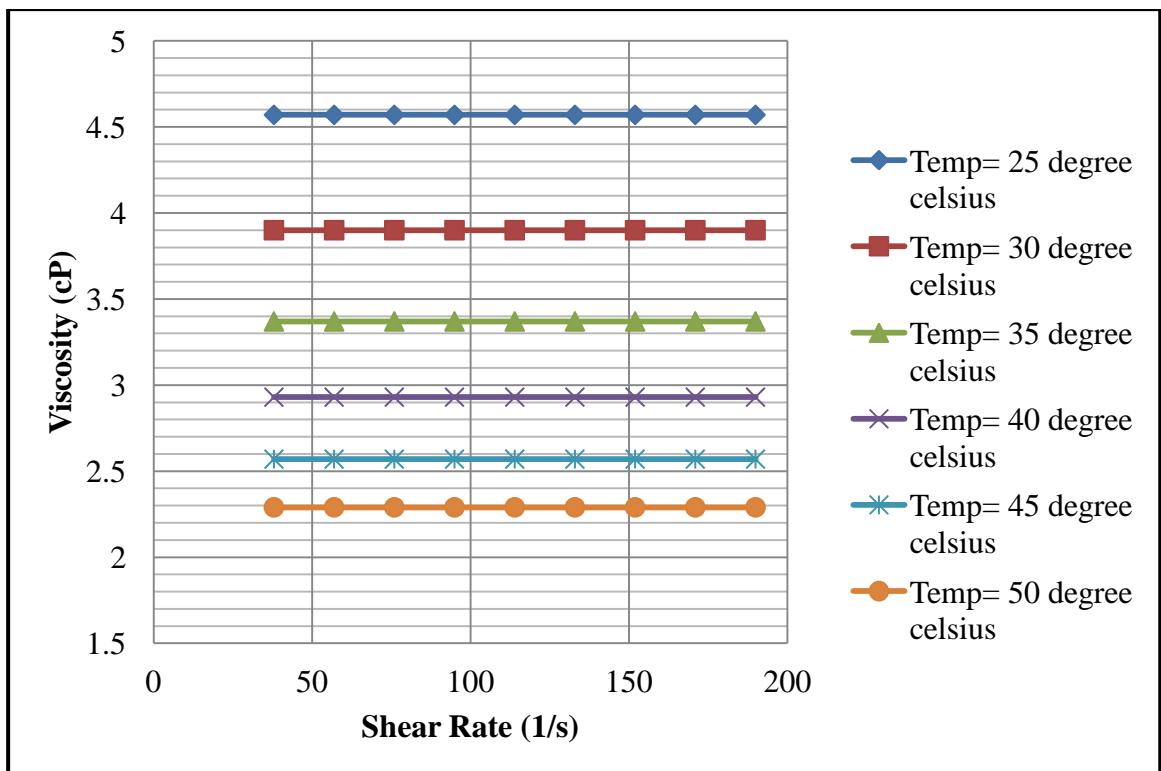


Figure 4.25 Viscosity versus shear rate of Al₂O₃ - (EG + H₂O) based nanofluid at a volumetric concentration of 0.05%

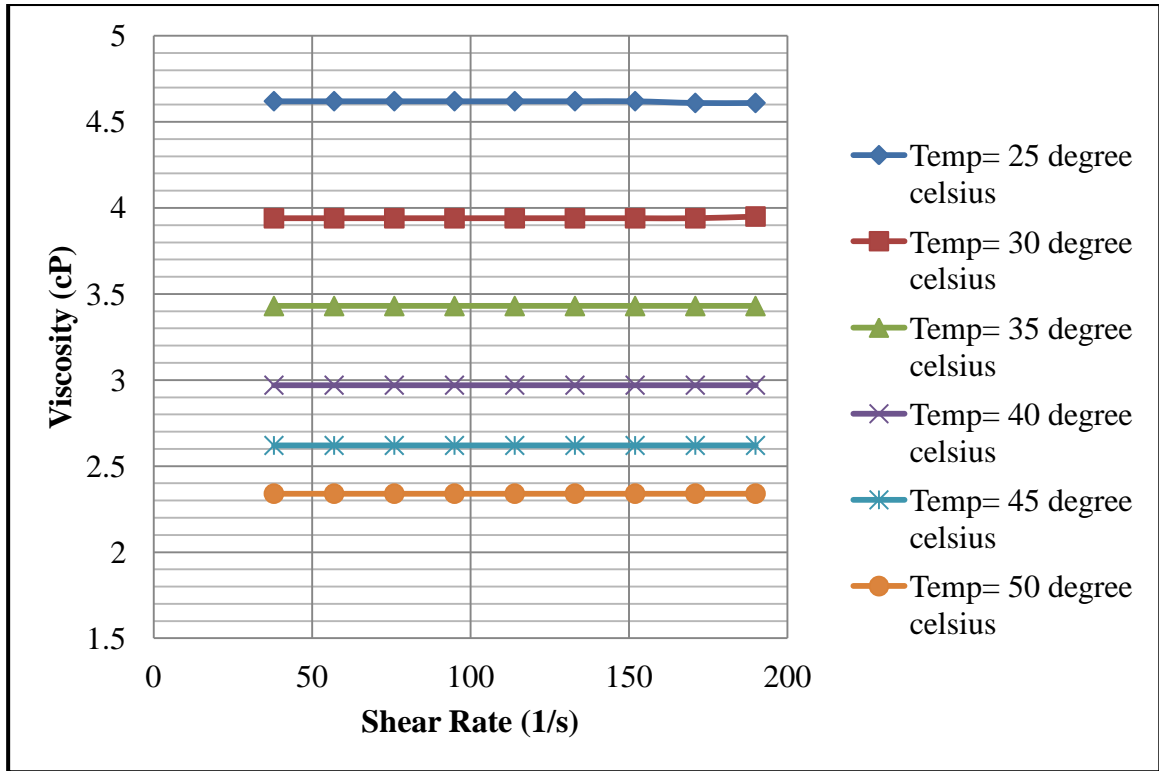


Figure 4.26 Viscosity versus shear rate of Al_2O_3 - (EG + H_2O) based nanofluid at a volumetric concentration of 0.1%

Figures 4.22 to 4.26 shows the variation of Viscosity with the Shear Rate at different volumetric concentrations of 0%, 0.005%, 0.01%, 0.05%, 0.1% of Al_2O_3 nanoparticles in ethylene glycol and water mixture as the base fluid and at different temperatures varied from 25 °C to 50 °C. As can be seen from the figure, that as the shear rate is varied in the range 0 to about 200 (1/s) for all the concentrations, the viscosity varies between 2 cP to about 5 cP for various concentrations and temperatures. It can also be seen, that at any temperature the viscosity lines are horizontal parallel to the horizontal axis. This implies that at any temperature, as the shear rate is increased the viscosity of the fluid remains constant. That is, the viscosity is independent of the shear rate applied. But, this is the condition of the Newtonian fluids. Therefore, the nanofluids considered, behaved as Newtonian. It can also be seen from the figure that at any concentration, the viscosity lines are horizontal at all the temperatures, but these horizontal viscosity lines are at different heights/ levels at different temperatures. This implies that the viscosity is varying with the temperature. And, at any concentration as the temperature increases the height of the lines decreases. The height represents the viscosity of the nanofluid; therefore with an increase in the temperature the viscosity gets decreased. The base fluid represents the case of 0% concentration and it is also behaving in the same manner as discussed above. Therefore,

we can conclude that the addition of Al_2O_3 nanoparticles in the concentrations of 0.005%, 0.01%, 0.05%, 0.1% in the (EG + H_2O) as base fluid did not changed its Newtonian behavior.

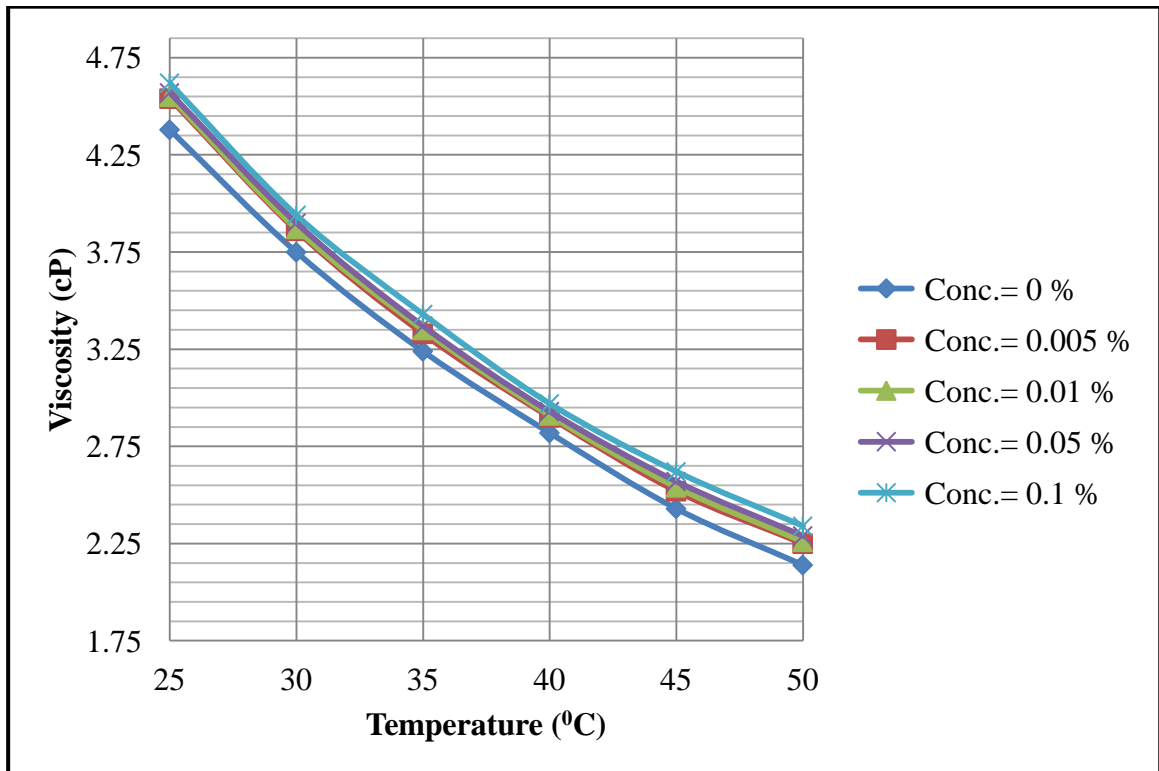


Figure 4.27 Viscosity versus temperature of Al_2O_3 - (EG + H_2O) based nanofluids at different volumetric concentrations (at a constant shear rate of 114 /s)

Figure 4.27 shows the variation of viscosity of nanofluids with the temperature at different volumetric concentrations of 0%, 0.005%, 0.01%, 0.05%, 0.1% of Al_2O_3 nanoparticles in ethylene glycol and water mixture as the base fluid and a constant shear rate of 114 (1/s). It can be seen from the figure that as the temperature is varied from 25 °C to 50 °C in steps of 5 °C the viscosity value varies between 2 cP to about 5 cP. That is, with an increase in temperature the viscosity decreases for each nanofluid concentration considered. This result was also clear from the figures 4.17 to 4.26. But actual variation i.e., whether the viscosity is decreasing linearly or non- linearly with an increase in temperature was not clear. Therefore to study the actual variation of viscosity with temperature, the graph between viscosity and temperature is plotted. Now, it is clear from the figure that the viscosity is decreasing non- linearly with an increase in temperature. It is also seen that the slope of the line decreases as the temperature is increased. The slope represents the rate of variation, therefore we can conclude that the rate of decrease of viscosity is more at the lower temperatures and gradually reduces as the temperature is increased. From the above

figure the viscosity variation at different concentrations is not clear, the curves seems to be overlapping. This is because in our experimental work we are dealing with lower concentrations, which affects the viscosity marginally. But if we see the experimental data in the tabular format given at the end in the annexure, it can be inferred that the higher concentration curves are above than the lower concentration curves.

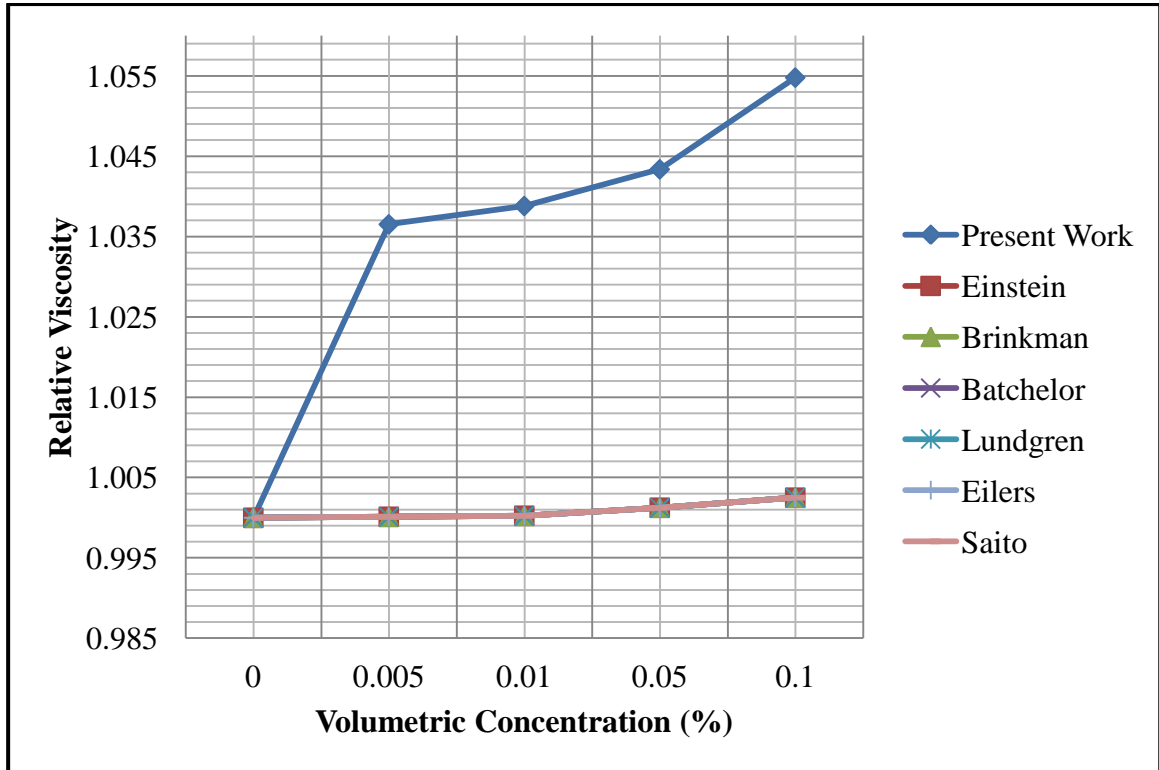


Figure 4.28 Relative viscosity versus volumetric concentration of Al_2O_3 - (EG + H_2O) based nanofluids (at a constant shear rate of 114 /s, constant temperature of 25 $^\circ\text{C}$) and its comparison with the theoretical models

As discussed before, the variation of viscosity with concentration was not clear from the figure 4.27. Therefore, to see the variation of viscosity with concentration and to compare with classical theoretical models, a new graph as shown in the figure 4.28 is drawn. Figure 4.28 represents the graph showing the variation of relative viscosity with volumetric concentration for the experimental work (at a constant shear rate of 114 /s and constant temperature of 25 $^\circ\text{C}$) and its comparison with different theoretical models. It can be easily seen from the figure that as the volumetric concentration increases the relative viscosity increases. The rate of increase of viscosity with concentration is almost linear for the volumetric concentrations increased from 0.005 % to 0.1 %. And, it also seen that the addition of 0.005 % of Al_2O_3 nanoparticles in (EG + H_2O) largely enhances the nanofluid viscosity as compared with other concentrations. It is seen that the theoretical models

largely underestimates the viscosity of nanofluids. And, their underestimation of the viscosity increases with an increase in the concentration. Therefore, we can conclude that there is a difference between the predicted and actual values of the viscosity and this difference increases with an increase in concentration.

4.5 Comparison of (EG) and (EG + H₂O) based nanofluids

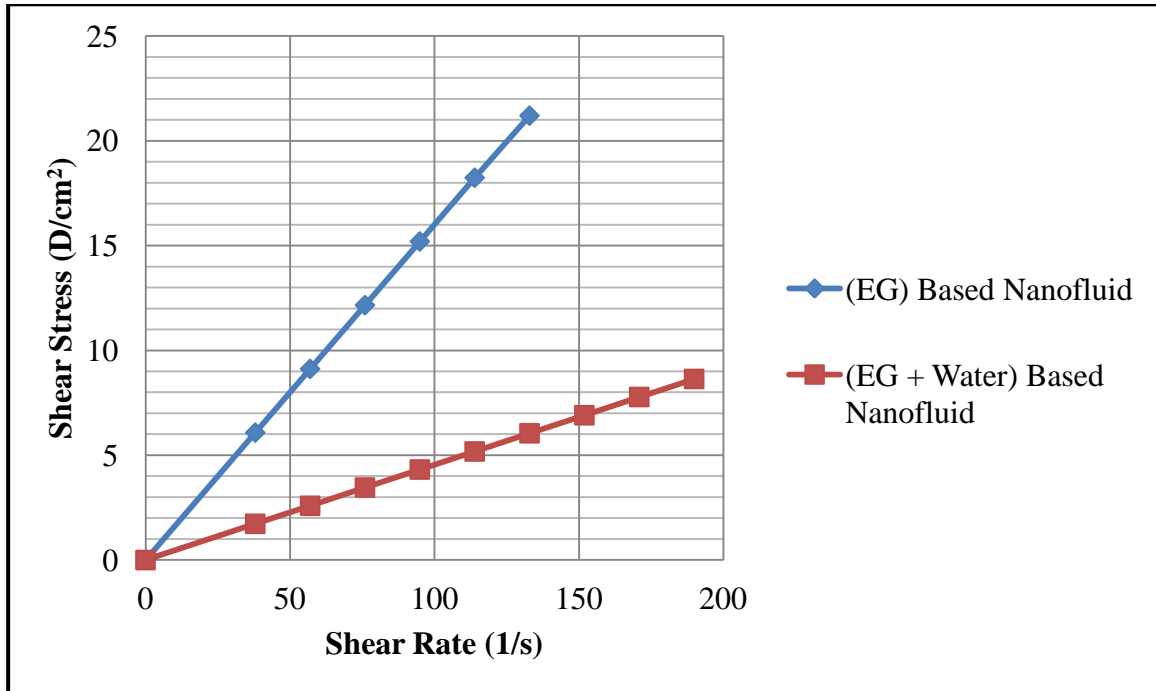


Figure 4.29 Shear stress versus shear rate at constant temperature of 25 °C for Al₂O₃ concentration of 0.01 % in (EG) and (EG + H₂O) as base fluid

Figure 4.29 shows the variation of shear stress with shear rate at constant temperature of 25 °C for Al₂O₃ concentration of 0.01 % in (EG) and (EG + H₂O) as base fluid. It is observed, that as the shear rate is varied in the range 0 to about 200 (1/s), the shear stress changes from about 0 to about 9 Dynes/ cm² for (EG + H₂O) based nanofluids. Whereas, for the (EG) based nanofluid the shear stress changes from about 0 to about 23 Dynes/ cm². It can be seen that as the shear rate is increased the shear stress developed in the fluid also increases. Therefore the shear stress is directly proportional to the shear rate. Therefore, both the Al₂O₃ - (EG + H₂O) and (EG) based nanofluids behaved as Newtonian. In the case of Newtonian fluids, the slope of the line represents the viscosity of nanofluids. As the slope of (EG) based nanofluid is more as compared to the slope of (EG + H₂O) based nanofluid, therefore it is concluded that the viscosity of (EG) based nanofluid is more than the (EG + H₂O) based nanofluid. And, both the nanofluids behaved as a Newtonian fluid in the same way as their respective base fluids.

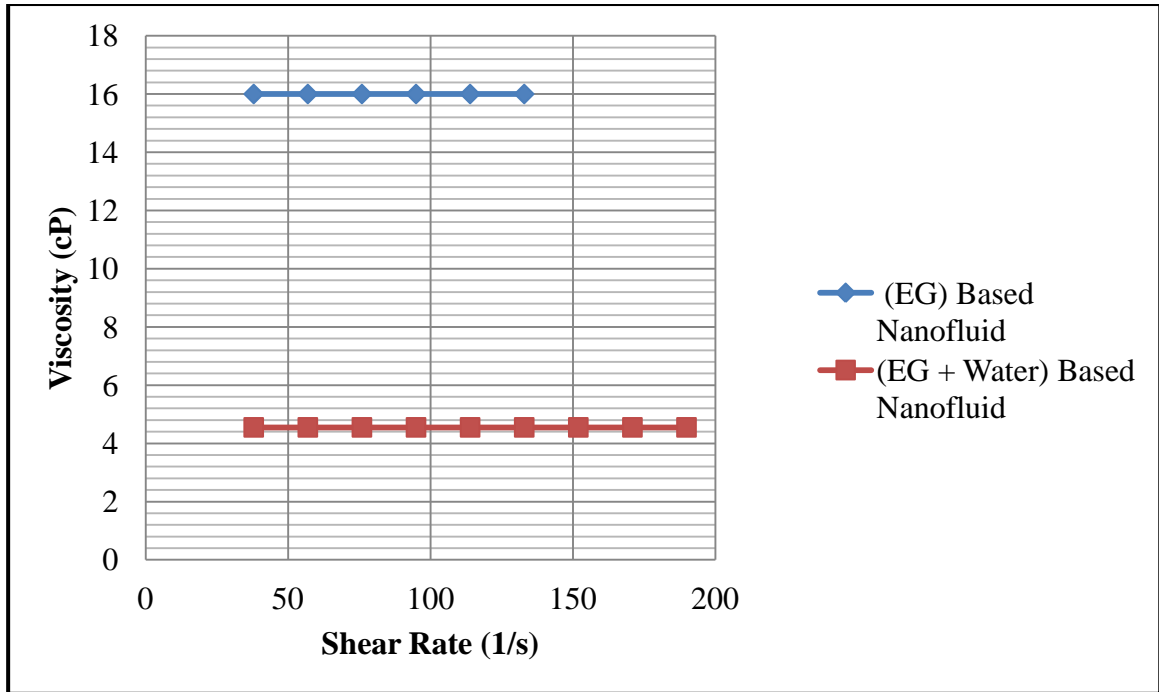


Figure 4.30 Viscosity versus shear rate of (EG) and (EG + H₂O) based nanofluids (at a constant temperature of 25 °C and a constant Al₂O₃ concentration of 0.01 %)

Figure 4.30 shows the viscosity comparison of (EG) and (EG + H₂O) based nanofluids with shear rate at a constant temperature of 25 °C and a constant Al₂O₃ concentration of 0.01 %. It can be seen from the graph that the viscosity remains constant with the change in shear rate for the respective nanofluids. That is, both the nanofluids behave as Newtonian in the same way as their respective base fluids. The constant viscosity value for the (EG) based nanofluid is more as compared to the (EG + H₂O) based nanofluid.

The viscosity of pure EG is 15.9 cP and the pure distilled water is 1 cP at 25 °C. When we mix EG in water in 60:40 ratio by volume, the value of viscosity is 4.38 cP at 25 °C. Although the viscosity was expected to be near about 10 cP i.e. more than the mid value of 1 cP and 15.9 cP, but its actual value is very much less than the mid value and it is 4.38 cP. Therefore, we cannot calculate the viscosity of the mixtures by taking average.

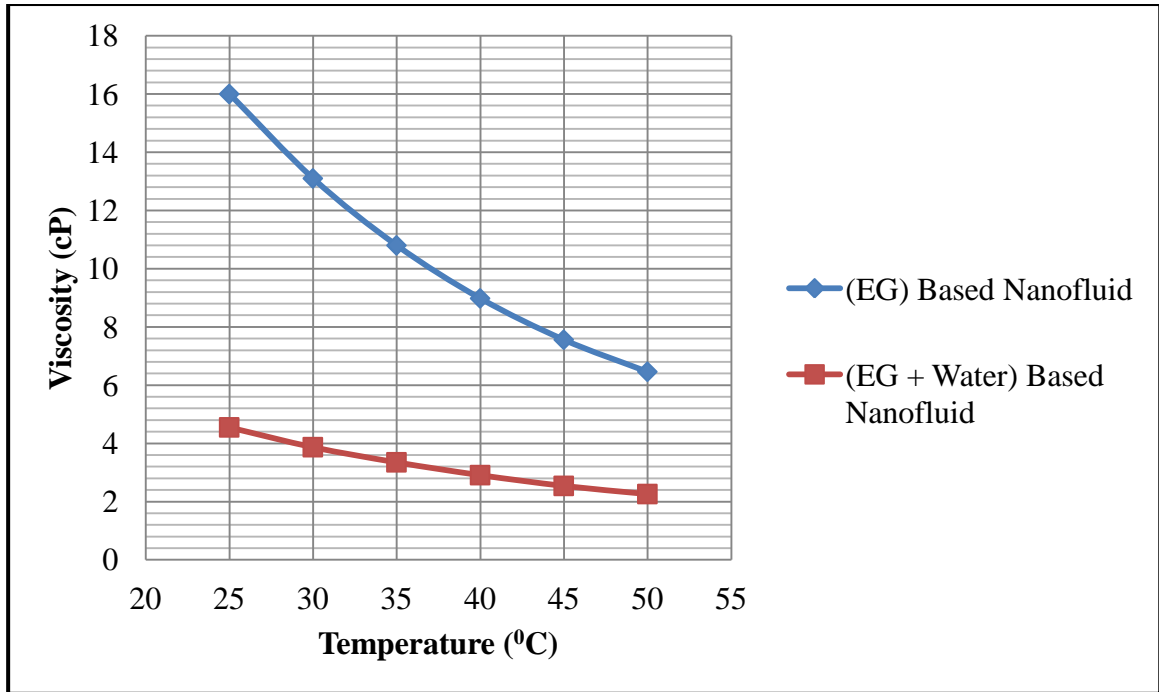


Figure 4.31 Viscosity versus temperature of (EG) and (EG + H₂O) based nanofluids (at a constant Al₂O₃ concentration of 0.01 % and a constant shear rate of 114 (1/s))

Figure 4.31 shows the viscosity comparison of (EG) and (EG + H₂O) based nanofluids with temperature at a constant Al₂O₃ concentration of 0.01 % and a constant shear rate of 114 (1/s). As can be seen from the figure, that as the temperature is increased from 25 °C to 50 °C the viscosity of both the nanofluids decreases. But, the slope of EG based nanofluid is more as compared to the (EG + H₂O) based nanofluid. Therefore, the rate of decrease in viscosity with an increase in temperature is more for the EG based naofluid as compared to the (EG + H₂O) based nanofluid. The viscosity varies from 16 cP at 25 °C to 6.46 cP at 50 °C for the (EG) based nanofluid. That is, for (EG) based nanofluid the range of viscosity variation is $16 - 6.46 = 9.54$ cP. The viscosity varies from 4.55 cP at 25 °C to 2.26 cP at 50 °C for the (EG + H₂O) based nanofluid. That is, for (EG + H₂O) based nanofluid the range of viscosity variation is $4.55 - 2.26 = 2.29$ cP. Therefore, it is concluded that the viscosity variation with temperature is more in (EG) based nanofluid as compared to the (EG + H₂O) based nanofluid. Therefore, for the same concentration, the rate of viscosity decrease with temperature is more in the case of nanofluids having base fluids of higher viscosity than the base fluids of lower viscosity. Therefore, the viscous behavior of the nanofluids strongly depends on the viscosity of the base fluid.

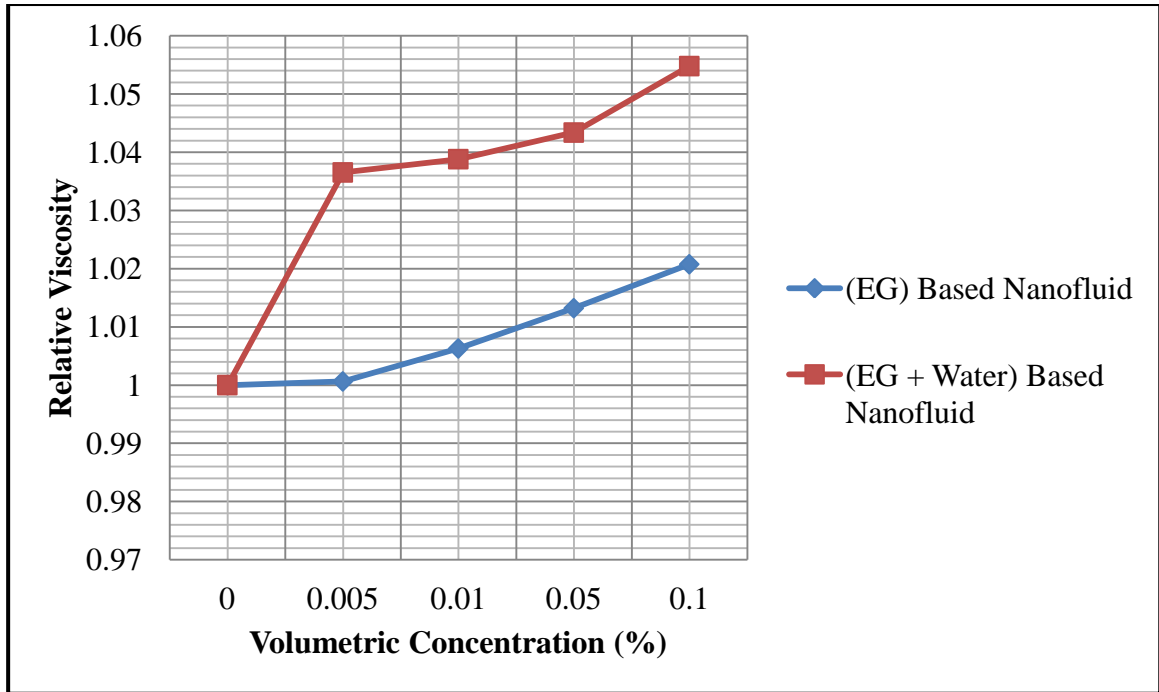


Figure 4.32 Relative viscosity versus concentration of (EG) and (EG + H₂O) based nanofluids (at a constant temperature of 25 °C and a constant shear rate of 114 (1/s))

Figure 4.32 shows the variation of relative viscosity of (EG) and (EG + H₂O) based nanofluids with concentration at a constant temperature of 25 °C and a constant shear rate of 114 (1/s). It can be seen from the figure that relative viscosity increases with the nanoparticle concentration for both the nanofluids. But, the enhancement of viscosity is more in case of (EG + H₂O) based nanofluids than the (EG) based nanofluid. That is, the effect of nanoparticles in enhancing the viscosity of the base fluid is more in the basefluids of lesser viscosity as compared to the basefluids of higher viscosity. The reason for this behavior is that the particle - fluid interactions are more in the case of a less viscous fluid than in the more viscous fluid. Also, the addition of 0.005 % of nanoparticles largely enhances the viscosity of (EG + H₂O) based nanofluid as compared to the (EG) based nanofluid. And, from 0.005 to 0.1% increase in concentration the viscosity increase is almost same in both the nanofluids.

CONCLUSIONS AND FUTURE SCOPE

5.1 Conclusions

- The viscous behavior of pure (EG) and (EG + H₂O) fluids is Newtonian, i.e. viscosity is unaffected by the shear rate applied in the range from 0 to about 200 (1/s).
- For the same applied shear rate range, the addition of the nanoparticles in the small volumetric concentrations of 0.005%, 0.01%, 0.05%, 0.1% in (EG) and (EG + H₂O) as the base fluid does not affect its rheological behavior i.e., the nanofluids retain their Newtonian behavior in the same way as their respective base fluids.
- The viscosity of (EG) and (EG + H₂O) based nanofluids decreases with an increase in the temperature from 25 °C to the 50 °C. As the temperature increases the fluid expands, that is its volume increases and molecules become loosely bound and their force of cohesion reduces. Therefore, due to their reduced cohesion, they offer less resistance to each other's movement, which ultimately reduces the viscosity.
- The rate of decrease of viscosity with an increase of temperature is non-linear for both the (EG) and (EG + H₂O) based nanofluids.
- For the same concentration, the rate of decrease of viscosity is more at the lower temperatures and gradually reduces as the temperature is increased.
- The rate of viscosity variation with temperature is more in (EG) based nanofluid as compared to the (EG + H₂O) based nanofluid.
- For the same concentration, the rate of viscosity decrease with temperature is more in case of nanofluids having base fluids of higher viscosity than the nanofluids having base fluids of lower viscosity. Hence, viscous behavior of the nanofluids strongly depends on the viscosity of the base fluid.
- The relative viscosity increases with the nanoparticle concentration for both the (EG) and (EG + H₂O) based nanofluids.
- The enhancement of viscosity with an increase of concentration is more in case of (EG + H₂O) based nanofluids than the (EG) based nanofluid.

- The effect of nanoparticles in enhancing the viscosity of the base fluid is more in the basefluids of lesser viscosity as compared to the basefluids of higher viscosity. The reason for this behavior is that the particle - fluid interactions are more in the case of less viscous fluid than in the case of a more viscous fluid.
- The theoretical models largely underestimates the viscosity of the (EG) and (EG + H₂O) based nanofluids.
- The conventional models such as Einstein model consider only the nanoparticles volume concentration for nanofluid viscosity prediction. But as discussed, the concentration is not the only factor that affects the viscosity; there are many other factors also that affect the viscosity of the nanofluids.

5.2 Future Scope

- It is useful for cold climate applications as EG which is antifreeze is used as a base fluid.
- As, the Sonication Time, Surfactants used, pH value of the fluid affects the stability of the nanofluids which in turn affects the viscosity. Hence, the effect of these factors on the viscosity of nanofluids should be studied.
- It will help to evaluate the heat transfer problems as Reynolds number and prandtl number are both functions of viscosity.
- For the study of pumping power requirements.
- Same technique can be used to study other nanofluids.

REFERENCES

- [1] Choi S.U.S., (1995), Enhancing thermal conductivity of fluids with nanoparticles, in: D.A. Singer, H.P. Wang (Eds.), *Developments and Applications of Non-Newtonian Flows*, FED 231/MD 66, ASME, New York, 99 - 105.
- [2] Das K. S., Choi S.U.S, Wenhua Yu and Pradeep T., (2007), *Nanofluids: Science and Technology*. John Wiley & Sons, Inc. New Jersey, 1 - 2.
- [3] Eastman J.A., Choi S.U.S., Li S., Thompson L.J., Lee S., (1997), Enhanced thermal conductivity through the development of nanofluids, *Materials Research Society Symposium- proceedings*, Materials Research Society, Pittsburgh, PA, USA, Boston, MA, USA, vol. 457, 3 - 11.
- [4] Lee S., Choi S.U.S., Li S., Eastman J.A., (1999), Measuring thermal conductivity of fluids containing oxide nanoparticles, *Journal of Heat Transfer* 121, 280 - 289.
- [5] Wang X., Xu X., Choi S.U.S., (1999), Thermal conductivity of nanoparticle–fluid mixture, *Journal of Thermophysics and Heat Transfer* 13 (4), 474 - 480.
- [6] Murshed S.M.S., Leong K.C., Yang C., (2005), Enhanced thermal conductivity of TiO₂–water based nanofluids, *International Journal of Thermal Sciences* 44 (4), 367 - 373.
- [7] Akoh H., Tsukasaki Y., Yatsuya S., Tasaki A., (1978), Magnetic properties of ferromagnetic ultrafine particles prepared by vacuum evaporation on running oil substrate, *Journal of Crystal Growth* 45, 495 - 500.
- [8] Zhu H., Lin Y., Yin Y., (2004), A novel one-step chemical method for preparation of copper nanofluids, *Journal of Colloid and Interface Science* 227, 100 - 103.
- [9] Krishnakumar S. and Somasundaran P., (1996), ESR investigations on the stabilization of alumina dispersions by Aerosol-OT in different solvents, *Colloids and Surfaces A: Physicochemical and Engineering Aspects*, 1 17(1), 37 - 44.
- [10] Chandrasekar M., Suresh S., Chandra Bose A., (2010), Experimental investigations and theoretical determination of thermal conductivity and viscosity of Al₂O₃/water nanofluid, *Experimental Thermal and Fluid Science* 34, 210 - 216.
- [11] Namburu P.K., Kulkarni D.P., Dandekar A. and Das D.K., (2007), Experimental investigation of viscosity and specific heat of silicon dioxide nanofluids, *Micro & Nano Letters*, 2 (3), 67 - 51.

- [12] Chen H., Ding Y., Lapkin A., Fan X., (2009), Rheological behaviour of ethylene glycol-titanate nanotube nanofluids, *J Nanopart Res* 11, 1513 - 1520.
- [13] Guo S.Z., Li Y., Jiang J.S., Xie H.Q., (2010), Nanofluids Containing α -Fe₂O₃ Nanoparticles and Their Heat Transfer Enhancements, *Nanoscale Res Lett* 5, 1222 - 1227.
- [14] Li X., Zhu D., Wang X., (2009), Experimental Investigation on Viscosity of Cu-H₂O Nanofluids, *Journal of Wuhan University of Technology - Mater. Sci. Ed.*, 24 (1), 48 - 52.
- [15] Kole M., Dey T.K., (2011), Effect of aggregation on the viscosity of copper oxide - gear oil nano fluids, *International Journal of Thermal Sciences* 50, 1741 - 1747.
- [16] Phuoc T.X., Massoudi M., (2009), Experimental observations of the effects of shear rates and particle concentration on the viscosity of Fe₂O₃-deionized water nanofluids, *International Journal of Thermal Sciences* 48, 1294 - 1301.
- [17] Duangthongsuk W., Wongwises S., (2009), Measurement of temperature-dependent thermal conductivity and viscosity of TiO₂ - water nanofluids, *Experimental Thermal and Fluid Science* 33, 706 - 714.
- [18] Garg P., Jorge L.A., Charles M., Thomas A.C., David A.K., Kalyan A., (2009), An experimental study on the effect of ultrasonication on viscosity and heat transfer performance of multi-wall carbon nanotube-based aqueous nanofluids, *International Journal of Heat and Mass Transfer* 52, 5090 - 5101.
- [19] Abareshi M., Sajjadi S.H., Zebarjad S.M., Goharshadi E.K., (2011), Fabrication, characterization, and measurement of viscosity of α -Fe₂O₃ -glycerol nano fluids, *Journal of Molecular Liquids* 163, 27 - 32.
- [20] Yu W., Xie H., Chen L., Li Y., (2009), Investigation of thermal conductivity and viscosity of ethylene glycol based ZnO nanofluid, *Thermochimica Acta* 491, 92 - 96.
- [21] Namburu P.K., Kulkarni D.P., Misra D., Das D.K., (2007), Viscosity of copper oxide nanoparticles dispersed in ethylene glycol and water mixture, *Experimental Thermal and Fluid Science* 32, 397 - 402.
- [22] Nguyen C.T., Desgranges F., Roy G., Galanis N., Mare T., Boucher S., Mintsa H.A., (2007), Temperature and particle-size dependent viscosity data for water-based nanofluids – Hysteresis phenomenon, *International Journal of Heat and Fluid Flow* 28, 1492 - 1506.

- [23] Jang S.P., Hwang K.S., Lee J.H., Kim J.H., Lee B.H. and Choi S. U.S., Choi C.J., (2008), Effective viscosities and thermal conductivities of aqueous nanofluids containing low volume concentrations of Al₂O₃ nanoparticles, *International Journal of Heat and Mass Transfer* 51, 2651 - 2656.
- [24] Wang X.J., Li X.F., (2009), Influence of pH on Nanofluids Viscosity and Thermal Conductivity, *CHIN. PHYS. LETT.* 26(5), 056601(1 - 4).
- [25] Duan F., Kwek D., Crivoi A., (2011), Viscosity affected by nanoparticle aggregation in Al₂O₃-water nanofluids, *Nanoscale Research Letters* 6:248, 1 - 5.
- [26] Einstein A., (1906), Eine neue Bestimmung der Moleküldimensionen, *Annalender Physik* 19, 289 - 306.
- [27] Brinkman H.C., (1952), The viscosity of concentrated suspensions and solution, *J. Chem. Phys.* 20, 571 - 581.
- [28] Frankel N.A., Acrivos A., (1967), On the viscosity of a concentrate suspension of solid spheres, *Chem. Engg. Sci.* 22, 847 - 853.
- [29] Lundgren T.S., (1972), Slow flow through stationary random beds and suspensions of spheres, *J. Fluid Mech.* 51, 273 - 299.
- [30] Batchelor G.K., (1977), The effect of Brownian motion on the bulk stress in a suspension of spherical particles, *J. Fluid Mech.* 83(1), 97 - 117.
- [31] Graham A.L., (1981), On the viscosity of suspensions of solid spheres, *Appl. Sci. Res.* 37, 275 - 286.
- [32] Eilers V.H., (1941), Die viskocitat von emulsionen hochviskoser stoffe als funktion der konzentration, *Kolloid-Zeitschrift* 97, 313 - 321.
- [33] Saito N., (1950), Concentration dependence of the viscosity of high polymer solutions, *J. Phys. Soc. Jpn.* 5, 4 - 8.

ANNEXURE- I

Table A.1 Experimental data of ethylene glycol at different temperatures and shear rates

Temp= 25 °C		
Shear Rate (1/s)	Viscosity (cP)	Shear Stress (D/cm ²)
38	15.9	6.04
57	15.9	9.06
76	15.9	12.1
95	15.9	15.1
114	15.9	18.12
133	15.9	21.14

Temp= 40 °C		
Shear Rate (1/s)	Viscosity (cP)	Shear Stress (D/cm ²)
38	8.91	3.38
57	8.91	5.07
76	8.91	6.77
95	8.91	8.46
114	8.91	10.15
133	8.91	11.85
152	8.91	13.54
171	8.91	15.23
190	8.91	16.92

Temp= 30 °C		
Shear Rate (1/s)	Viscosity (cP)	Shear Stress (D/cm ²)
38	13	4.94
57	13	7.41
76	13	9.87
95	13	12.35
114	13	14.82
133	13	17.29
152	13	19.76
171	13	22.23

Temp= 45 °C		
Shear Rate (1/s)	Viscosity (cP)	Shear Stress (D/cm ²)
38	7.47	2.83
57	7.47	4.26
76	7.47	5.66
95	7.47	7.09
114	7.47	8.51
133	7.47	9.94
152	7.47	11.35
171	7.47	12.77
190	7.47	14.19

Temp= 35 °C		
Shear Rate (1/s)	Viscosity (cP)	Shear Stress (D/cm ²)
38	10.71	4.07
57	10.71	6.11
76	10.71	8.13
95	10.71	10.17
114	10.71	12.2
133	10.71	14.24
152	10.71	16.28
171	10.71	18.32
190	10.71	20.35

Temp= 50 °C		
Shear Rate (1/s)	Viscosity (cP)	Shear Stress (D/cm ²)
38	6.36	2.41
57	6.36	3.62
76	6.36	4.83
95	6.36	6.04
114	6.36	7.25
133	6.36	8.46
152	6.36	9.67
171	6.36	10.88
190	6.36	12.08

ANNEXURE- II

Table A.2 Experimental data of Al₂O₃ - ethylene glycol based nanofluid at a volumetric concentration of 0.005% at different temperatures and shear rates

Temp= 25 °C		
Shear Rate (1/s)	Viscosity (cP)	Shear Stress (D/cm ²)
38	15.92	6.05
57	15.92	9.1
76	15.92	12.12
95	15.92	15.11
114	15.91	18.14
133	15.91	21.17

Temp= 40 °C		
Shear Rate (1/s)	Viscosity (cP)	Shear Stress (D/cm ²)
38	8.93	3.39
57	8.93	5.09
76	8.93	6.78
95	8.93	8.48
114	8.93	10.18
133	8.93	11.88
152	8.92	13.57
171	8.92	15.25
190	8.92	16.96

Temp= 30 °C		
Shear Rate (1/s)	Viscosity (cP)	Shear Stress (D/cm ²)
38	13.02	4.95
57	13.02	7.42
76	13.02	9.88
95	13.02	12.37
114	13.01	14.84
133	13.01	17.3
152	13.02	19.8
171	13.01	22.25

Temp= 45 °C		
Shear Rate (1/s)	Viscosity (cP)	Shear Stress (D/cm ²)
38	7.49	2.85
57	7.49	4.27
76	7.49	5.69
95	7.48	7.11
114	7.48	8.54
133	7.48	9.96
152	7.48	11.38
171	7.48	12.81
190	7.48	14.23

Temp= 35 °C		
Shear Rate (1/s)	Viscosity (cP)	Shear Stress (D/cm ²)
38	10.73	4.08
57	10.73	6.12
76	10.73	8.15
95	10.73	10.19
114	10.72	12.23
133	10.73	14.27
152	10.72	16.31
171	10.72	18.35
190	10.72	20.38

Temp= 50 °C		
Shear Rate (1/s)	Viscosity (cP)	Shear Stress (D/cm ²)
38	6.38	2.42
57	6.38	3.63
76	6.38	4.85
95	6.38	6.06
114	6.38	7.27
133	6.38	8.48
152	6.38	9.7
171	6.38	10.91
190	6.37	12.12

ANNEXURE- III

Table A.3 Experimental data of Al₂O₃ - ethylene glycol based nanofluid at a volumetric concentration of 0.01% at different temperatures and shear rates

Temp= 25 °C		
Shear Rate (1/s)	Viscosity (cP)	Shear Stress (D/cm ²)
38	16	6.08
57	16	9.12
76	16	12.16
95	16	15.2
114	16	18.24
133	16	21.2

Temp= 40 °C		
Shear Rate (1/s)	Viscosity (cP)	Shear Stress (D/cm ²)
38	8.98	3.41
57	8.98	5.12
76	8.98	6.83
95	8.98	8.53
114	8.98	10.24
133	8.98	11.94
152	8.98	13.65
171	8.97	15.36
190	8.97	17.06

Temp= 30 °C		
Shear Rate (1/s)	Viscosity (cP)	Shear Stress (D/cm ²)
38	13.1	4.98
57	13.1	7.47
76	13.1	9.96
95	13.1	12.45
114	13.1	14.93
133	13.1	17.42
152	13.1	19.91
171	13.1	22.4

Temp= 45 °C		
Shear Rate (1/s)	Viscosity (cP)	Shear Stress (D/cm ²)
38	7.56	2.87
57	7.56	4.31
76	7.56	5.75
95	7.56	7.18
114	7.56	8.62
133	7.56	10.05
152	7.56	11.49
171	7.56	12.93
190	7.55	14.36

Temp= 35 °C		
Shear Rate (1/s)	Viscosity (cP)	Shear Stress (D/cm ²)
38	10.8	4.1
57	10.8	6.16
76	10.8	8.21
95	10.8	10.26
114	10.8	12.31
133	10.8	14.36
152	10.79	16.42
171	10.79	18.47
190	10.79	20.52

Temp= 50 °C		
Shear Rate (1/s)	Viscosity (cP)	Shear Stress (D/cm ²)
38	6.46	2.45
57	6.46	3.68
76	6.46	4.91
95	6.46	6.14
114	6.46	7.36
133	6.46	8.59
152	6.46	9.82
171	6.45	11.05
190	6.45	12.27

ANNEXURE- IV

Table A.4 Experimental data of Al₂O₃ - ethylene glycol based nanofluid at a volumetric concentration of 0.05% at different temperatures and shear rates

Temp= 25 °C		
Shear Rate (1/s)	Viscosity (cP)	Shear Stress (D/cm ²)
38	16.12	6.13
57	16.12	9.19
76	16.12	12.25
95	16.12	15.31
114	16.11	18.38
133	16.11	21.44

Temp= 40 °C		
Shear Rate (1/s)	Viscosity (cP)	Shear Stress (D/cm ²)
38	9.1	3.46
57	9.1	5.19
76	9.1	6.92
95	9.1	8.64
114	9.1	10.37
133	9.1	12.1
152	9.09	13.83
171	9.09	15.56
190	9.09	17.29

Temp= 30 °C		
Shear Rate (1/s)	Viscosity (cP)	Shear Stress (D/cm ²)
38	13.21	5.02
57	13.21	7.53
76	13.21	10.04
95	13.21	12.55
114	13.21	15.06
133	13.21	17.57
152	13.21	20.08
171	13.2	22.59

Temp= 45 °C		
Shear Rate (1/s)	Viscosity (cP)	Shear Stress (D/cm ²)
38	7.66	2.91
57	7.66	4.37
76	7.66	5.82
95	7.66	7.28
114	7.66	8.73
133	7.66	10.19
152	7.66	11.64
171	7.66	13.1
190	7.65	14.55

Temp= 35 °C		
Shear Rate (1/s)	Viscosity (cP)	Shear Stress (D/cm ²)
38	10.89	4.14
57	10.89	6.21
76	10.89	8.28
95	10.89	10.35
114	10.89	12.42
133	10.89	14.48
152	10.89	16.55
171	10.88	18.62
190	10.88	20.69

Temp= 50 °C		
Shear Rate (1/s)	Viscosity (cP)	Shear Stress (D/cm ²)
38	6.57	2.5
57	6.57	3.74
76	6.57	4.99
95	6.57	6.24
114	6.57	7.49
133	6.57	8.74
152	6.57	9.98
171	6.57	11.23
190	6.57	12.48

ANNEXURE- V

Table A.5 Experimental data of Al₂O₃ - ethylene glycol based nanofluid at a volumetric concentration of 0.1% at different temperatures and shear rates

Temp= 25 °C		
Shear Rate (1/s)	Viscosity (cP)	Shear Stress (D/cm ²)
38	16.23	6.17
57	16.23	9.25
76	16.23	12.33
95	16.23	15.42
114	16.23	18.5
133	16.22	21.58

Temp= 40 °C		
Shear Rate (1/s)	Viscosity (cP)	Shear Stress (D/cm ²)
38	9.19	3.49
57	9.19	5.24
76	9.19	6.98
95	9.19	8.73
114	9.19	10.48
133	9.19	12.22
152	9.19	13.97
171	9.18	15.71
190	9.18	17.46

Temp= 30 °C		
Shear Rate (1/s)	Viscosity (cP)	Shear Stress (D/cm ²)
38	13.33	5.06
57	13.33	7.6
76	13.33	10.13
95	13.33	12.66
114	13.33	15.19
133	13.33	17.73
152	13.32	20.26
171	13.32	22.79

Temp= 45 °C		
Shear Rate (1/s)	Viscosity (cP)	Shear Stress (D/cm ²)
38	7.78	2.96
57	7.78	4.43
76	7.78	5.91
95	7.78	7.39
114	7.78	8.87
133	7.78	10.35
152	7.78	11.82
171	7.78	13.3
190	7.77	14.78

Temp= 35 °C		
Shear Rate (1/s)	Viscosity (cP)	Shear Stress (D/cm ²)
38	10.98	4.17
57	10.98	6.26
76	10.98	8.34
95	10.98	10.43
114	10.98	12.52
133	10.98	14.6
152	10.98	16.69
171	10.98	18.8
190	10.97	20.86

Temp= 50 °C		
Shear Rate (1/s)	Viscosity (cP)	Shear Stress (D/cm ²)
38	6.68	2.54
57	6.68	3.81
76	6.68	5.08
95	6.68	6.35
114	6.68	7.6
133	6.68	8.88
152	6.68	10.15
171	6.68	11.42
190	6.67	12.69

ANNEXURE- VI

Table A.6 Experimental data of EG and H₂O mixture in 60:40 ratio by volume at different temperatures and shear rates

Temp= 25 °C		
Shear Rate (1/s)	Viscosity (cP)	Shear Stress (D/cm ²)
38	4.38	1.66
57	4.38	2.49
76	4.38	3.33
95	4.38	4.16
114	4.38	4.99
133	4.38	5.82
152	4.37	6.66
171	4.37	7.49
190	4.37	8.32

Temp= 40 °C		
Shear Rate (1/s)	Viscosity (cP)	Shear Stress (D/cm ²)
38	2.82	1.07
57	2.82	1.61
76	2.82	2.14
95	2.82	2.68
114	2.82	3.21
133	2.82	3.75
152	2.82	4.28
171	2.82	4.82
190	2.81	5.36

Temp= 30 °C		
Shear Rate (1/s)	Viscosity (cP)	Shear Stress (D/cm ²)
38	3.75	1.42
57	3.75	2.14
76	3.75	2.85
95	3.75	3.56
114	3.75	4.27
133	3.75	4.99
152	3.75	5.7
171	3.74	6.4
190	3.74	7.12

Temp= 45 °C		
Shear Rate (1/s)	Viscosity (cP)	Shear Stress (D/cm ²)
38	2.43	0.92
57	2.43	1.38
76	2.43	1.85
95	2.43	2.31
114	2.43	2.77
133	2.43	3.23
152	2.43	3.69
171	2.43	4.15
190	2.43	4.62

Temp= 35 °C		
Shear Rate (1/s)	Viscosity (cP)	Shear Stress (D/cm ²)
38	3.24	1.23
57	3.24	1.85
76	3.24	2.46
95	3.24	3.08
114	3.24	3.69
133	3.24	4.31
152	3.23	4.93
171	3.23	5.54
190	3.23	6.16

Temp= 50 °C		
Shear Rate (1/s)	Viscosity (cP)	Shear Stress (D/cm ²)
38	2.14	0.81
57	2.14	1.22
76	2.14	1.63
95	2.14	2.03
114	2.14	2.44
133	2.14	2.85
152	2.14	3.25
171	2.14	3.66
190	2.14	4.07

ANNEXURE- VII

Table A.7 Experimental data of Al₂O₃ -(EG and H₂O mixture) based nanofluid at a volumetric concentration of 0.005% at different temperatures and shear rates

Temp= 25 °C		
Shear Rate (1/s)	Viscosity (cP)	Shear Stress (D/cm ²)
38	4.54	1.72
57	4.54	2.58
76	4.54	3.45
95	4.54	4.31
114	4.54	5.17
133	4.54	6.04
152	4.54	6.9
171	4.54	7.76
190	4.54	8.62

Temp= 40 °C		
Shear Rate (1/s)	Viscosity (cP)	Shear Stress (D/cm ²)
38	2.9	1.1
57	2.9	1.65
76	2.9	2.2
95	2.9	2.75
114	2.9	3.3
133	2.9	3.86
152	2.9	4.41
171	2.9	4.96
190	2.9	5.51

Temp= 30 °C		
Shear Rate (1/s)	Viscosity (cP)	Shear Stress (D/cm ²)
38	3.86	1.46
57	3.86	2.2
76	3.86	2.93
95	3.86	3.67
114	3.86	4.4
133	3.86	5.13
152	3.86	5.87
171	3.86	6.6
190	3.86	7.33

Temp= 45 °C		
Shear Rate (1/s)	Viscosity (cP)	Shear Stress (D/cm ²)
38	2.52	0.96
57	2.52	1.44
76	2.52	1.92
95	2.52	2.39
114	2.52	2.87
133	2.52	3.35
152	2.52	3.83
171	2.52	4.31
190	2.52	4.79

Temp= 35 °C		
Shear Rate (1/s)	Viscosity (cP)	Shear Stress (D/cm ²)
38	3.33	1.26
57	3.33	1.89
76	3.33	2.53
95	3.33	3.16
114	3.33	3.8
133	3.33	4.43
152	3.33	5.06
171	3.33	5.7
190	3.33	6.33

Temp= 50 °C		
Shear Rate (1/s)	Viscosity (cP)	Shear Stress (D/cm ²)
38	2.25	0.85
57	2.25	1.28
76	2.25	1.71
95	2.25	2.14
114	2.25	2.56
133	2.25	2.99
152	2.25	3.42
171	2.25	3.85
190	2.25	4.27

ANNEXURE- VIII

Table A.8 Experimental data of Al₂O₃ - (EG and H₂O mixture) based nanofluid at a volumetric concentration of 0.01% at different temperatures and shear rates

Temp= 25 °C		
Shear Rate (1/s)	Viscosity (cP)	Shear Stress (D/cm ²)
38	4.55	1.73
57	4.55	2.59
76	4.55	3.46
95	4.55	4.32
114	4.55	5.18
133	4.55	6.05
152	4.55	6.91
171	4.55	7.78
190	4.55	8.64

Temp= 40 °C		
Shear Rate (1/s)	Viscosity (cP)	Shear Stress (D/cm ²)
38	2.91	1.1
57	2.91	1.66
76	2.91	2.21
95	2.91	2.76
114	2.91	3.32
133	2.91	3.87
152	2.91	4.42
171	2.91	4.98
190	2.91	5.53

Temp= 30 °C		
Shear Rate	Viscosity	Shear Stress
38	3.87	1.47
57	3.87	2.21
76	3.87	2.94
95	3.87	3.68
114	3.87	4.41
133	3.87	5.14
152	3.87	5.88
171	3.87	6.62
190	3.87	7.35

Temp= 45 °C		
Shear Rate (1/s)	Viscosity (cP)	Shear Stress (D/cm ²)
38	2.54	0.97
57	2.54	1.45
76	2.54	1.93
95	2.54	2.41
114	2.54	2.9
133	2.54	3.38
152	2.54	3.86
171	2.53	4.34
190	2.53	4.82

Temp= 35 °C		
Shear Rate (1/s)	Viscosity (cP)	Shear Stress (D/cm ²)
38	3.35	1.27
57	3.35	1.91
76	3.35	2.54
95	3.35	3.18
114	3.35	3.82
133	3.35	4.45
152	3.35	5.09
171	3.34	5.72
190	3.34	6.35

Temp= 50 °C		
Shear Rate (1/s)	Viscosity (cP)	Shear Stress (D/cm ²)
38	2.26	0.86
57	2.26	1.29
76	2.26	1.72
95	2.26	2.15
114	2.26	2.58
133	2.26	3
152	2.26	3.44
171	2.26	3.86
190	2.25	4.29

ANNEXURE- IX

Table A.9 Experimental data of Al₂O₃ - (EG and H₂O mixture) based nanofluid at a volumetric concentration of 0.05% at different temperatures and shear rates

Temp= 25 °C		
Shear Rate (1/s)	Viscosity (cP)	Shear Stress (D/cm ²)
38	4.57	1.74
57	4.57	2.6
76	4.57	3.47
95	4.57	4.34
114	4.57	5.2
133	4.57	6.08
152	4.57	6.95
171	4.57	7.81
190	4.57	8.7

Temp= 40 °C		
Shear Rate (1/s)	Viscosity (cP)	Shear Stress (D/cm ²)
38	2.93	1.11
57	2.93	1.67
76	2.93	2.23
95	2.93	2.78
114	2.93	3.34
133	2.93	3.9
152	2.93	4.45
171	2.93	5
190	2.93	5.57

Temp= 30 °C		
Shear Rate (1/s)	Viscosity (cP)	Shear Stress (D/cm ²)
38	3.9	1.48
57	3.9	2.22
76	3.9	2.96
95	3.9	3.7
114	3.9	4.45
133	3.9	5.19
152	3.9	5.93
171	3.9	6.67
190	3.9	7.41

Temp= 45 °C		
Shear Rate (1/s)	Viscosity (cP)	Shear Stress (D/cm ²)
38	2.57	0.98
57	2.57	1.46
76	2.57	1.95
95	2.57	2.44
114	2.57	2.93
133	2.57	3.42
152	2.57	3.9
171	2.57	4.39
190	2.57	4.88

Temp= 35 °C		
Shear Rate (1/s)	Viscosity (cP)	Shear Stress (D/cm ²)
38	3.37	1.28
57	3.37	1.92
76	3.37	2.56
95	3.37	3.2
114	3.37	3.84
133	3.37	4.48
152	3.37	5.12
171	3.37	5.76
190	3.37	6.4

Temp= 50 °C		
Shear Rate (1/s)	Viscosity (cP)	Shear Stress (D/cm ²)
38	2.29	0.87
57	2.29	1.31
76	2.29	1.74
95	2.29	2.18
114	2.29	2.61
133	2.29	3.04
152	2.29	3.48
171	2.29	3.91
190	2.29	4.35

ANNEXURE- X

Table A.10 Experimental data of Al₂O₃ - (EG and H₂O mixture) based nanofluid at a volumetric concentration of 0.1% at different temperatures and shear rates

Temp= 25 °C		
Shear Rate (1/s)	Viscosity (cP)	Shear Stress (D/cm ²)
38	4.62	1.76
57	4.62	2.63
76	4.62	3.51
95	4.62	4.39
114	4.62	5.27
133	4.62	6.14
152	4.62	7
171	4.61	7.9
190	4.61	8.78

Temp= 40 °C		
Shear Rate (1/s)	Viscosity (cP)	Shear Stress (D/cm ²)
38	2.97	1.13
57	2.97	1.69
76	2.97	2.26
95	2.97	2.82
114	2.97	3.39
133	2.97	3.95
152	2.97	4.51
171	2.97	5.08
190	2.97	5.64

Temp= 30 °C		
Shear Rate (1/s)	Viscosity (cP)	Shear Stress (D/cm ²)
38	3.94	1.5
57	3.94	2.25
76	3.94	2.99
95	3.94	3.74
114	3.94	4.49
133	3.94	5.24
152	3.94	6
171	3.94	6.74
190	3.95	7.49

Temp= 45 °C		
Shear Rate (1/s)	Viscosity (cP)	Shear Stress (D/cm ²)
38	2.62	1
57	2.62	1.49
76	2.62	1.99
95	2.62	2.49
114	2.62	2.99
133	2.62	3.48
152	2.62	3.98
171	2.62	4.48
190	2.62	4.98

Temp= 35 °C		
Shear Rate (1/s)	Viscosity (cP)	Shear Stress (D/cm ²)
38	3.43	1.3
57	3.43	1.95
76	3.43	2.6
95	3.43	3.26
114	3.43	3.9
133	3.43	4.56
152	3.43	5.21
171	3.43	5.87
190	3.43	6.52

Temp= 50 °C		
Shear Rate (1/s)	Viscosity (cP)	Shear Stress (D/cm ²)
38	2.34	0.89
57	2.34	1.33
76	2.34	1.78
95	2.34	2.22
114	2.34	2.66
133	2.34	3.11
152	2.34	3.56
171	2.34	4
190	2.34	4.45